

Collapse and accretion of ancient seamounts : a
Jurassic example from the Mino terrane, the
Suzuka Mountains, central Japan

山縣, 毅

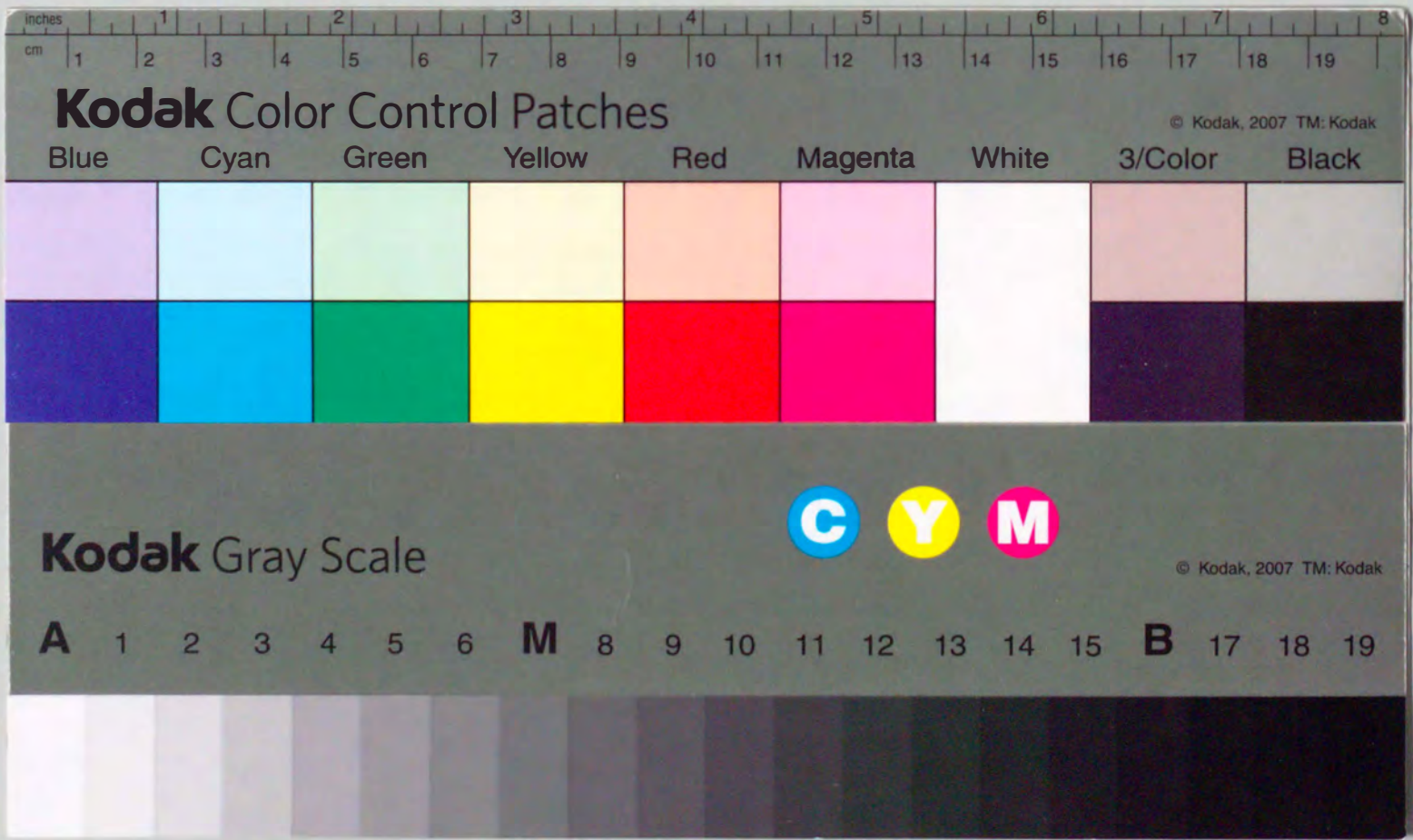
<https://doi.org/10.11501/3075545>

出版情報 : 九州大学, 1993, 博士 (理学), 論文博士
バージョン :
権利関係 :

Collapse and accretion of ancient seamounts

--a Jurassic example from the Mino terrane, the Suzuka Mountains, central Japan--

山 縣 毅



①

**Collapse and accretion of ancient seamounts
—a Jurassic example from the Mino terrane,
the Suzuka Mountains, central Japan—**

Takeshi YAMAGATA

Abstract

The major purpose of this thesis is to discuss the collapse and accretionary processes of an ancient seamount and associated sediments. Chosen for this study is the Permian oceanic-rocks occurring as a huge rock-body in the Jurassic terrigenous rocks of the Mino terrane in the northern Suzuka Mountains, central Japan. The description focuses on the internal textural destruction of the Permian oceanic rocks and their chaotic intermixing.

Rocks of the Mino terrane in the study area were grouped into two major tectonostratigraphic units; the Suzuka unit defined as an aggregate of diverse oceanic rocks chiefly of Permian age and subordinately of Jurassic age and the Hikone unit labeled as lower Upper Jurassic olistostromes. The former is at present separated from the latter by thrust faults, but was primarily in a block-in-matrix contact with the latter. The Suzuka unit is labeled as a huge exotic rock-body chiefly underlain by and partly embedded in the Hikone unit.

The stratigraphic reconstruction reveals that the Suzuka oceanic rocks are divided into five lithologic successions. They comprise the upper Lower Permian shallow marine limestone succession, upper Lower Permian allochthonous limestone succession, Lower Permian chert succession, basaltic rock succession, and Jurassic siliceous rock succession. It is stressed that no coarse terrigenous clastic grains are contaminated in the five successions. The stratigraphic, petrographic, and paleontologic examinations have revealed that the Permian oceanic rocks were formed as sediments on and around a basaltic seamount.

The field examination shows that the Suzuka oceanic rocks were stratally disrupted

into numerous, isolated masses set in a matrix of mechanically crushed, fine-grained basaltic materials. The oceanic rock masses widely range in size from a few millimeters to a few kilometers or more and are completely disorganized, randomly distributed without any structural trends.

The microscopic observation identifies the mechanical, internal destruction of primary textures of the basaltic rocks occurring as isolated masses. The destruction is characterized by the pervasive and penetrative brecciation in a brittle manner. The rare ductile deformation is represented by injection of finely pulverized materials. The same destruction fabrics are identified in the fine-grained basaltic materials that form the matrix enclosing the oceanic-rock blocks. The Suzuka unit comprises a lithologically heterogeneous aggregate of stratally disrupted and internally crushed oceanic rocks which are chaotically intermixed with one another.

The prevailing internal destruction of the basaltic rocks and chaotic intermixing of the oceanic rocks can be best explained by a large-scaled collapse of a seamount and associated sediments along a convergent margin. Such a large-scaled collapse is most likely to have been induced by block-faulting of the seamount on an outer trench-slope. During the downslope-movement of the collapsed products towards a trench, various-sized oceanic-rock masses and finely crushed basaltic materials were chaotically mingled with each other. The wedge of disrupted oceanic rocks was gravitationally emplaced down onto trench-fill sediments and then incorporated into an accretionary prism. All these tectonic events are considered to have taken place in the late Middle to early Late Jurassic time.

Contents

I. Introduction	1
II. Geologic setting	4
A. Geologic outline of Mino terrane	4
B. Previous works and geologic framework in northern Suzuka Mountains	6
III. Method of study and terminology	10
A. Method of study	10
B. Terminology	11
IV. Stratigraphy and age of oceanic-rocks of Suzuka unit	11
A. Basaltic rock succession	15
B. Permian shallow-marine limestone succession	17
1. Lithostratigraphy	17
2. Age	20
3. Limestone-types	22
C. Permian allochthonous limestone succession	26
1. Lithostratigraphy	26
2. Age	31
D. Permian chert succession	33
1. Lithology	33
2. Age	33
E. Jurassic siliceous rock succession	33
1. Lithostratigraphy	33
2. Age	37
V. Internal textural destruction of Suzuka oceanic rocks and their chaotic intermixing	37

A. Internal textural destruction of basaltic rocks -----	38
1. Weak destruction fabric -----	41
2. Moderate destruction fabric -----	43
3. Strong destruction fabric -----	44
B. Chaotic intermixing of oceanic-rock blocks of Suzuka unit-----	45
VI. Structural relationship of Permian oceanic rocks to Jurassic terrigenous sediments-----	50
VII. Discussion -----	54
A. Reconstruction of depositional setting of Permian oceanic rocks-----	54
1. Shallow-marine limestone succession -----	55
2. Allochthonous limestone succession -----	56
3. Chert succession -----	58
4. Reconstruction of depositional setting of Permian oceanic rocks -----	59
B. Mechanisms of internal destruction of basaltic rocks and intermixing of oceanic rocks -----	60
1. Internal destruction of basaltic rocks -----	61
2. Intermixing of oceanic rocks -----	63
C. Genesis of mixture of Permian oceanic rocks and Jurassic terrigenous sediments -----	65
D. Formation process of Suzuka unit -----	66
VIII. Summary -----	68
IX. Acknowledgements -----	70
X. References -----	71

Plates 1 to 20

I. Introduction

Numerous seamounts are distributed on the modern ocean floors. Approximately one thousand of seamounts are reported in the western Pacific Ocean. Some of these modern seamounts are being collided to and subducted beneath forearc wedges of accretionary prisms in the modern trenches; the Japan Trench (Cadet *et al.*, 1987; Lallemand and Le Pichon, 1987; Kobayashi *et al.*, 1987; Yamazaki and Okamura, 1989), the Izu-Ogasawara Trench (Fryer and Smoot, 1985; Okamura *et al.*, 1992), the New Hebrides Trench (Fisher, 1986; Collot and Fisher, 1989). These seamounts have been split and fractured by block faulting along outer slopes of trenches (Fryer and Smoot, 1985; Cadet *et al.*, 1987). Breccias and blocks derived from seamounts are being deposited at the foot of fault-scarps and on the trench floors (Lallemand *et al.*, 1989; Pautot *et al.*, 1987). Some of the breccias and blocks have been accreted in the landward slope of the trench (i.e., the Daiichi-Kashima Seamount in the Japan Trench : Kobayashi *et al.*, 1987). However, most parts of those seamounts have been totally subducted beneath forearc wedges, not having been detached from the oceanic floor nor obducted onto the forearc wedges. Only top parts of the seamounts are known to have been detached and incorporated into accretionary prisms of forearc wedges (Okamura, 1991). Magnetic anomalies and morphologic features indicate the presence of previously subducted seamounts beneath forearc wedges at the junction of the Japan and Kuril Trenches (Lallemand and Le Pichon, 1987; Yamazaki and Okamura, 1989), in the Nankai Trough (Okamura and Joshima, 1986; Yamazaki and Okamura, 1989), and in the New Hebrides Trench (Collot and Fisher, 1989).

On the other hand, ancient accretionary prisms often include huge masses of oceanic rocks reconstructed as remnant of seamounts (Akiyoshi terrane: Sano and

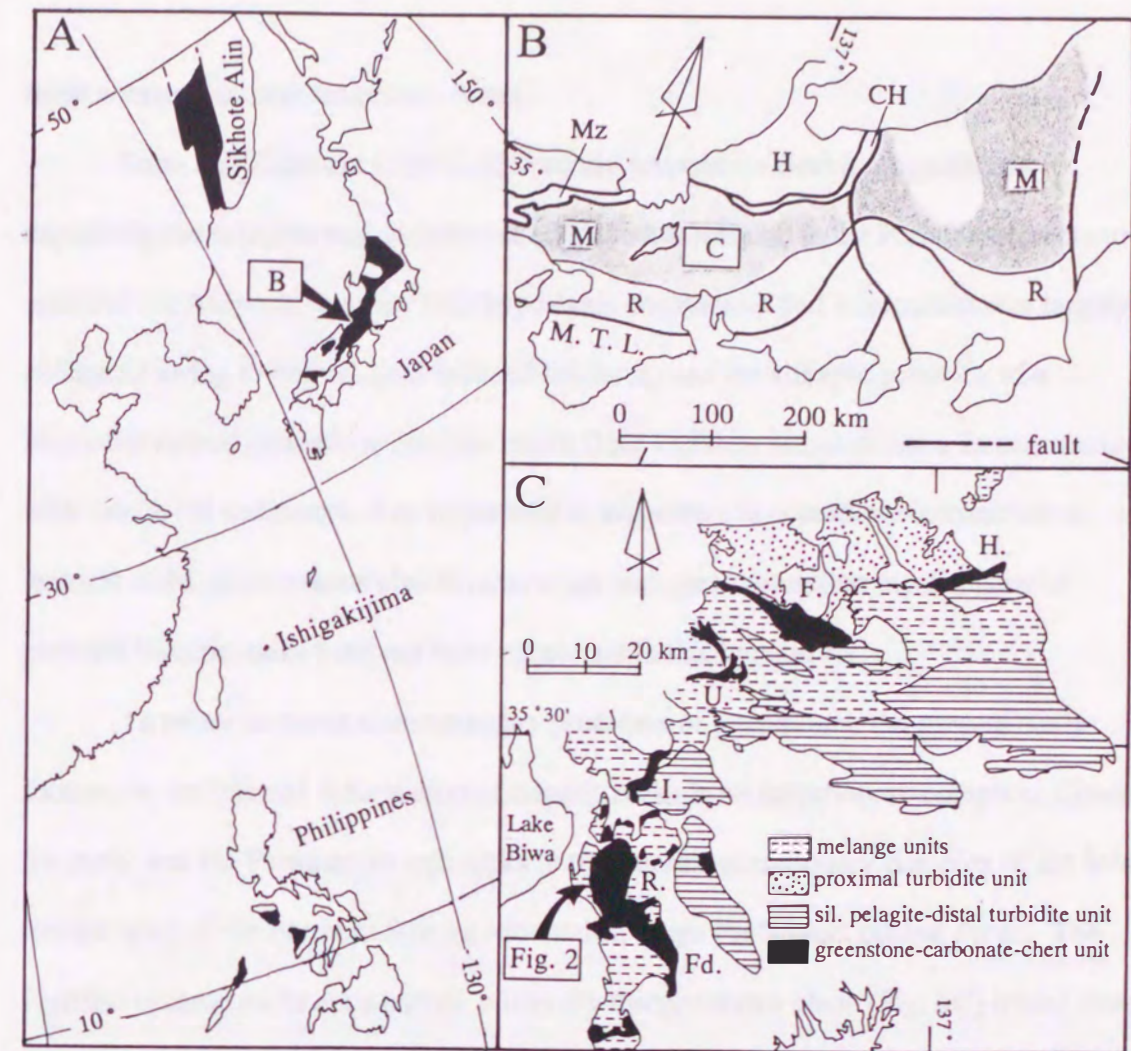


Fig. 1 Index maps showing geographic (A), tectonic (B), and tectonostratigraphic (C) of the Mino terrane. CH: Circum-Hida Tectonic Zone, H: Hida terrane, M: Mino terrane, Mz: Maizuru terrane, R: Ryoke metamorphic terrane, M.T.L.: Medium Tectonic Line. H: Hachiman, F: Funabuseyama, U: Uokaneyama, I: Ibukiyama, R: Ryozen, Fd.: Fujiwaradake.

Kanmera, 1988; Mino terrane : Sano, 1988 a ; Horibo, 1990). Much of these huge masses is exposed as allochthonous thrust-sheets resting on terrigenous rocks (Akiyoshi terrane: Kanmera and Nishi, 1983; Sano *et al.*, 1987; Mino terrane: Yamamoto, 1985; Sano, 1988 a ; Miyamura *et al.*, 1976; Harayama *et al.*, 1989). Therefore, it is controversial whether the accretion model of modern seamounts can simply be applied to



these accreted ancient seamounts or not.

Sano and Kanmera (1991a, d) recently proposed a working hypothesis explaining the collision and accretion of an ancient seamount in the Permian accretionary prism of the Akiyoshi terrane. This hypothesis emphasizes that a seamount was largely collapsed owing to normal fault-induced fracturing and the collapse products of a seamount moved downslope onto the trench floor and then accreted into a forearc wedge with trench-fill sediments. The hypothesis is suggestive to accretion mechanisms of tectonic slabs of seamounts also in other areas and ages. Accretion mechanisms of pedestal basaltic rocks have not been concerned in this hypothesis.

To better understand accretionary processes of a seamount, the present study focuses on the internal deformation of basaltic rocks in an accretionary complex. Chosen for study was the Permian oceanic rocks in the Jurassic accretionary complex of the Mino terrane lying in the northern Suzuka Mountains, Shiga Prefecture, central Japan. The Permian oceanic rocks are a part of a laterally discontinuous chain (Fig. 1C) traced from Hachiman (Wakita, 1984; Horibo, 1990), Funabuseyama (Kawai, 1964; Sano, 1988 a, b, c, d), Uokaneyama (Yamamoto, 1985), Ibukiyama (Yamamoto, 1985), and Ryozensan (Miyamura *et al.*, 1976) to Fujiwaradake (Murata, 1960; Harayama *et al.*, 1989) and have a chaotic structure characterized by Permian limestone blocks unsystematically embedded in basaltic rocks, which may be related to collision and accretion of a seamount.

It can be concluded that accreted oceanic rocks in the northern Suzuka Mountains are of a complicated aggregate of masses of basaltic rocks, limestones, and siliceous rocks. These oceanic rocks are considered to have primarily formed as a Permian basaltic seamount capped by shallow-marine limestone and covered by deep-marine siliceous sediments on its foot in an open-ocean realm. Microscopic examination shows that the

primary textures of basaltic rocks have been internally destroyed in a brittle manner and the destruction fabrics are pervasive and penetrative. Careful field observation reveals that these oceanic rocks have been complexly intermixed with Jurassic terrigenous sediments mainly at the marginal part of the unit. Formation of the aggregation of oceanic rocks masses, internal destruction in basaltic rocks, and mixing of oceanic rocks and terrigenous sediments are best explained by a huge collapse of a seamount onto a trench floor filled with terrigenous sediments, which is induced by progressive inclining of a normal fault-split seamount. Then, the collapse products are interpreted to have been accreted with the trench-fill terrigenous sediments into the Jurassic accretionary prisms.

II. Geologic setting

A. Geologic outline of Mino terrane

Mizutani and Hattori (1983) have defined the Mino terrane as the Mesozoic terrane composed of a heterogeneous assemblage of unmetamorphosed, upper Paleozoic and Mesozoic rocks in the continental side of southwest Japan. The northern correlative of the Mino terrane is described in Sikhote-Alin (Nadanhada-Western Sikhote-Alin: Kojima, 1989). Southern correlatives are found in the Philippines (North Palawan Block: Isozaki et al., 1988; Faure and Ishida, 1990) and Ishigakijima Island (Isozaki et al., 1989). The Mino terrane and its northern and southern correlatives form a belt of the Jurassic accretionary rocks fringing the eastern continental margin of Asia (Fig. 1A).

In central Japan where the Mino terrane rocks best crop out, the northern margin of the Mino terrane is tectonically bounded by the Circum-Hida Tectonic Zone, and the Maizuru terrane (Fig. 1B). In the south of the Mino terrane, the rocks gradually grade into the Ryoke metamorphic terrane.

A great deal of recent radiolarian biostratigraphic works (Wakita, 1988; Otsuka, 1988) as well as geological studies have completely revised the tectonostratigraphy and age of the Mino terrane rocks, much of which was previously believed to be the Carboniferous and Permian. According to the tectonostratigraphy recently proposed by Sano *et al.* (1992), the Mesozoic and Paleozoic rocks of the Mino terrane can be grouped into four units (Fig. 1C); (1) Permian greenstone-carbonate-chert unit, (2) Lower Triassic to lowest Cretaceous siliceous pelagite-distal turbidite unit, (3) Middle Jurassic proximal turbidite unit, and (4) upper Lower Jurassic to lowest Cretaceous melange unit. Sano *et al.* (1992) interpret these four units to be (1) sediments on and around a seamount in an open-ocean realm, (2) sediments accumulated in a pelagic realm to trench floor setting, in ascending order, (3) sediments deposited in a trench-slope basin, and (4) submarine slide deposits on a trench floor, respectively. Geochemical investigation shows that the volcanism setting of basaltic rocks of the greenstone-carbonate-chert unit was most likely a spreading axis-centered oceanic plateau or ridge (Jones *et al.*, 1993).

All these rocks form southerly-vergent, imbricated, complexly stacked structural wedges and show a southward younging polarity (Sano *et al.*, 1992; Wakita, 1988; Otsuka, 1988; Yamagata, 1989). Moreover, palaeomagnetic examinations of the Mesozoic pelagic sediments and Permian basaltic rocks (Hattori and Hirooka, 1977, 1979; Shibuta and Sasajima, 1980; Hattori, 1982) have revealed that these rocks accumulated in low-latitude areas far away to the south of the present position. All lines of evidence indicate that the sedimentary complex of the Mino terrane was formed by collision of the Permian to Jurassic oceanic rocks and their offscraping accretion together with Jurassic to earliest Cretaceous terrigenous sediments in a trench area (Sano *et al.*, 1992).

B. Previous works and geologic framework in northern Suzuka Mountains

Miyamura *et al.* (1976) were the first to examine the stratigraphy of rocks of the Mino terrane in the Suzuka Mountains and have divided the Mino terrane rocks into the Ikuridani, Hikone, and Kitasuzuka Groups. The Ikuridani Group is composed of sandstone, black mudstone, and chert intercalating limestone lens. The Hikone Group was lithologically subdivided into the lower Mitigadani and upper Maihara Formations. The Mitigadani Formation is composed mainly of black mudstone containing lenticular beds of chert, and the Maihara Formation comprises black mudstone and chert with a small amount of sandstone. The Kitasuzuka Group was subdivided into the lower

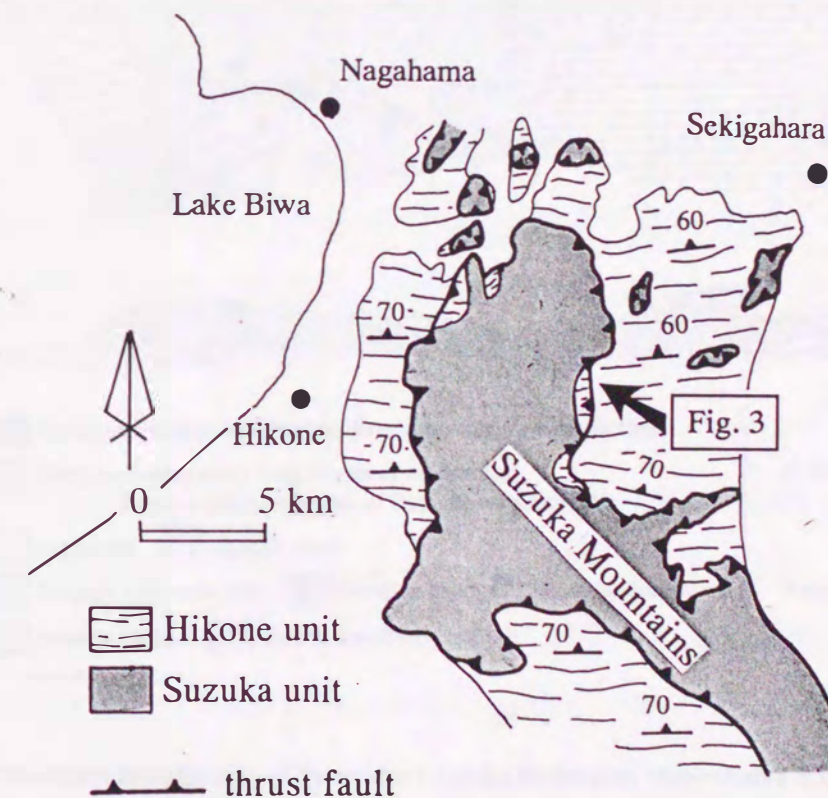


Fig. 2 Tectonostratigraphic sketch map of the Suzuka Mountains. Map area is indicated in Fig. 1C.

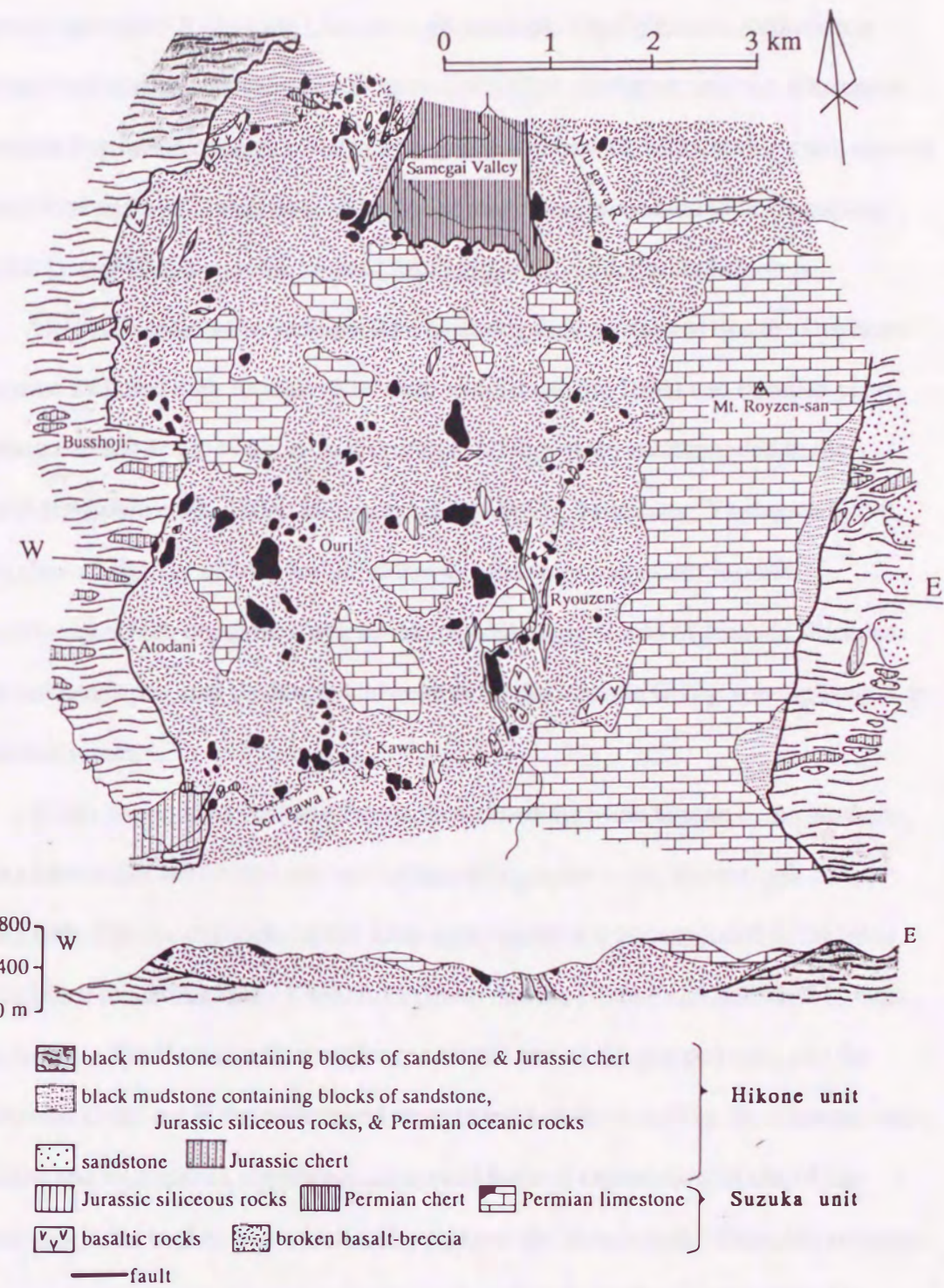


Fig. 3 Tectonostratigraphic map of the northern Suzuka Mountains. Mapped area is shown in Fig. 2.

Ojigahata and upper Ryozensan Limestone Formations. The Ojigahata Formation is composed of predominant chert which intercalates black mudstone, and the Ryozensan Limestone Formation consists mainly of limestone and basaltic rocks with a small amount of sandstone and black mudstone. The three groups were presumed to be correlated with the Lower Permian on the basis of fusuline fossils yielded from limestone.

However, radiolarian and conodont biostratigraphies revealed that the Ojigahata Formation included both Jurassic (Kurimoto and Kuwahara, 1991) and Permian chert (Suetsugu, 1981) and the Hikone and Ikuridani Groups were corresponded to the Jurassic (Okimura *et al.*, 1986; Harayama *et al.*, 1989). Moreover, Yamagata (1990, 1993) showed that the Hikone and Ikuridani Groups were early Late Jurassic olistostromes, which comprise black mudstone containing blocks of Jurassic siliceous rocks and sandstone, and the black mudstone of the Kitasuzuka Group was equivalent to the olistostromes.

In this paper, Mesozoic and Paleozoic rocks of the Mino terrane in the northern Suzuka Mountains are divided into two tectonostratigraphic units; Hikone unit and Suzuka unit. The oceanic rocks of the Kitasuzuka Group are corresponded to the latter, and the black mudstone of the Kitasuzuka Group and the Hikone and Ikuridani Groups to the former. The Suzuka unit occupies the central part of the mapped area, and the Hikone unit crops out in the eastern and western parts of the area (Fig. 3). Though less extensive and widespread, significant are several isolated exposures of rocks of the Hikone unit in the central area underlain by rocks of the Suzuka unit. These Mino terrane rocks have been severely sheared and deformed, and penetrated and unconformably covered by less deformed, Late Cretaceous rhyolitic rocks (Koto Rhyolites: Mimura and Kawada, 1970).

The Suzuka unit chiefly comprises Permian basaltic rocks, limestone, and chert

with a small amount of Jurassic siliceous rocks, all having an oceanic affinity (Fig. 3). Except for occurrence of the Jurassic siliceous rocks, the lithologic association is almost identical to that of the greenstone-limestone-chert unit of Sano *et al.* (1992). In spite of the similarity in the lithologic association, the Suzuka unit much differs in stratal continuity from the rock-units referred to as the greenstone-limestone-chert unit. The primary stratigraphy of oceanic rocks of the Suzuka unit has been largely disrupted to form various-sized and often isolated blocks. Some of the large-sized blocks record parts of the primary stratigraphy. Thus the primary stratigraphy can be reconstructed by piecing together from isolated outcrops in the large-sized blocks.

The Hikone unit is characterized by dominance of black mudstone which has abundant blocks of sandstone and chert and related siliceous mudstone. The lithologic association as well as the deformation style means that the Hikone unit is referred to as olistostrome-slump unit of Sano *et al.* (1992). The black mudstone yields radiolarian fossils of the *Tricolocapsa conexa* zone indicative of early Late Jurassic (Yamagata, 1990, 1993).

Black mudstone is sandy and in places has thin sandy laminae. The scaly cleavage is penetrative and pervasive in black mudstone. Sandstone and siliceous rocks occur as laterally discrete, slab-, lenticular- and pod-shaped, isolated blocks embedded in black mudstone. These blocks have primarily irregular-rugged outlines and lithologically sharp boundaries to the surrounding black mudstone. The size of the blocks ranges from a few tens of centimeters to several tens of meters. The orientation of the blocks as well as the direction of the scaly cleavage means an east-west structural trend of the rocks of the Hikone unit.

The Suzuka unit tectonically overlies the Hikone unit, which in plan view surrounds the Suzuka unit (Fig. 2). The two units are at many localities in fault contact.

The boundaries between the two units nearly run north-south. Each of the eastern and western boundaries is gently inclined to the west and to the east, respectively (Fig. 3). To be noted is the structurally discordant relation of the boundaries to the general structural trend of rocks of the Hikone unit. The boundaries are oblique to the general structural trend of the Hikone rocks with a high angle.

In spite of the fault contact of the two units at many places, the careful field examination reveals that the two units were primarily in unshered contact with each other. Though structural aspect of the primary contact has not been fully understood, significant is that the rocks of the two units have been complexly intermixed to form a tectonite having a mylonitic appearance along the boundaries. The unshered contact as well as the mylonitic appearance rock along the boundaries implies a large-scaled gravitational sliding of the rocks of the Suzuka unit on the rocks of the Hikone unit, when the latter still unconsolidated.

III. Method of study and terminology

A. Method of study

The purpose of this paper is to discuss the collapse and accretionary process of an ancient seamount in the northern Suzuka Mountains. Owing to this purpose, the description focuses on the mega- to micro-scope structures of the Permian oceanic rocks of the Suzuka unit. Moreover, to understand these structures, the original stratigraphy of the oceanic rocks is reconstructed.

The concrete descriptions are followed:

- (1) distribution and mode of occurrence of oceanic rocks in a field.
- (2) lithology and internal deformation of oceanic rocks under the microscope

(3) fusuline biostratigraphy in limestone

(4) relationship of oceanic rocks to terrigenous rocks in a field and under the microscope.

B. Terminology

In this paper, some specific terms are used because of extremely chaotic structures of oceanic rocks of the Suzuka unit. Definitions of these terms are as follows.

unit: tectonostratigraphic unit comprising a mixture of lithostratigraphic units resulting from tectonic deformation.

succession: lithostratigraphic unit unified by consisting dominantly of a certain lithologic type.

member: lithostratigraphic unit is a part of a succession and possesses lithologic features distinguishing it from adjacent parts of the succession.

block and clast: rock fragments resulting from breaking of the parent mass of a lithostratigraphic unit. Simply in terms of the size, two varieties of rock-fragments are termed as blocks and clasts. The former is defined as a rock-mass larger than 10 cm in size and the latter as a smaller rock mass than 10 cm. This classification is not genetic, but simply based upon the size.

broken basalt-breccia: breccia consisting mainly of clasts of basaltic rocks having internal destruction fabrics with a matrix of fine destruction products of basaltic rocks. This term is newly coined in this study.

IV. Stratigraphy and age of oceanic rocks of Suzuka unit

The primary stratigraphy of the Suzuka oceanic rocks was reconstructed by

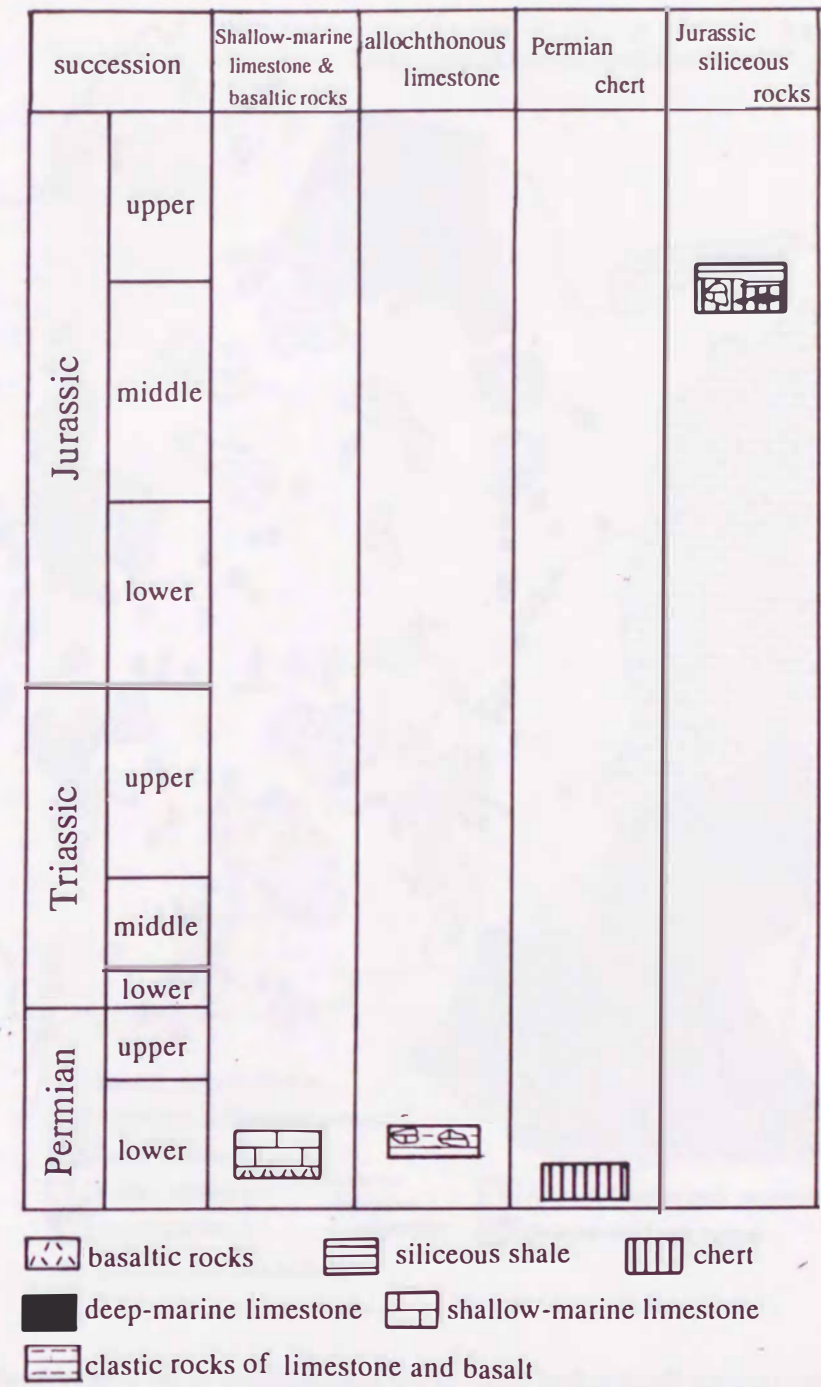


Fig. 4 The stratigraphy and ages of shallow-marine limestone, basaltic rocks, allochthonous limestone, Permian chert, and Jurassic siliceous rocks of the Suzuka unit.

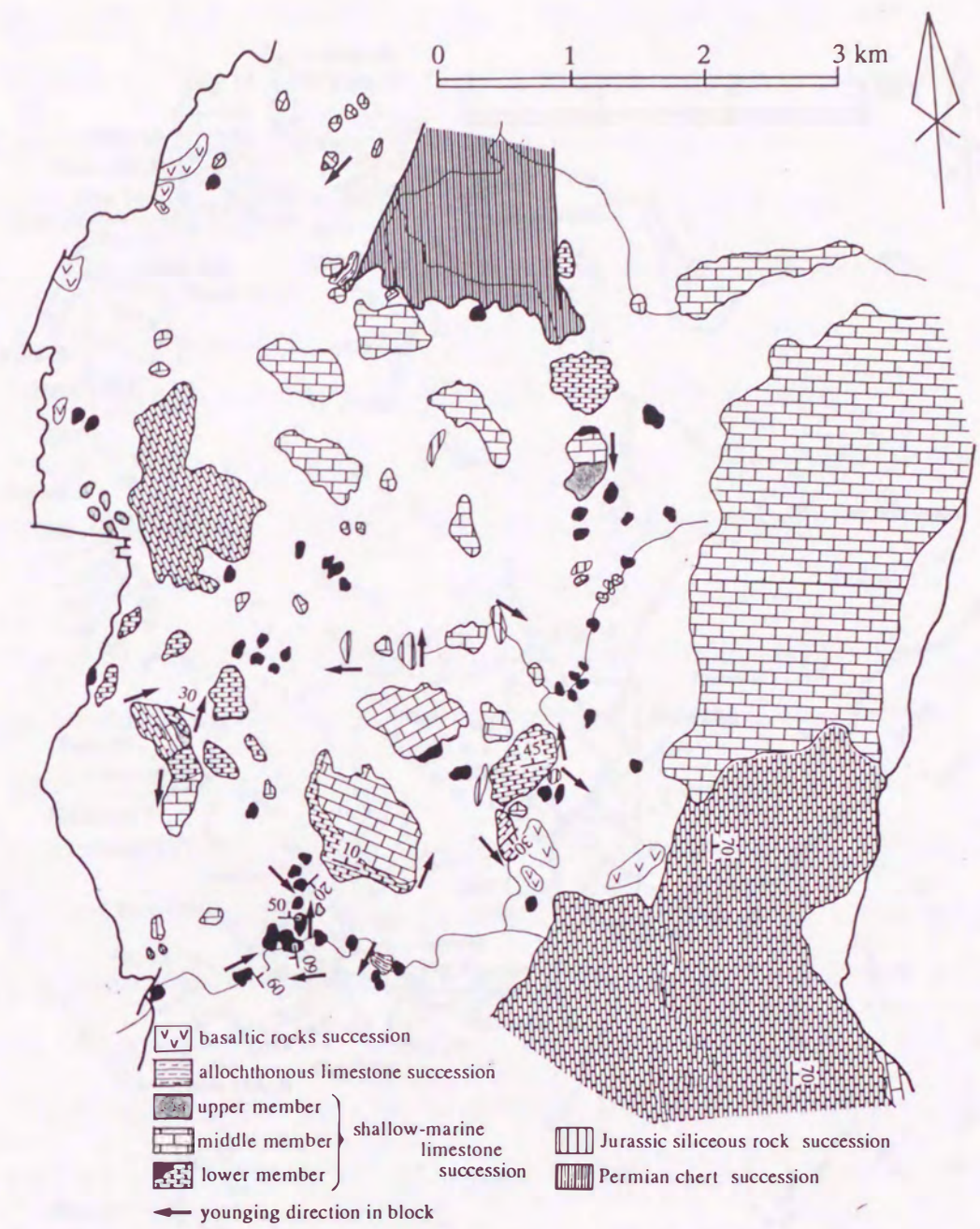


Fig. 5 Distribution of major mappable-sized blocks within broken basalt-breccia (white). In the blocks, the primary stratigraphy of shallow-marine limestone, basaltic rocks, allochthonous limestone, Permian chert, and Jurassic siliceous rocks are entirely or partly recorded.

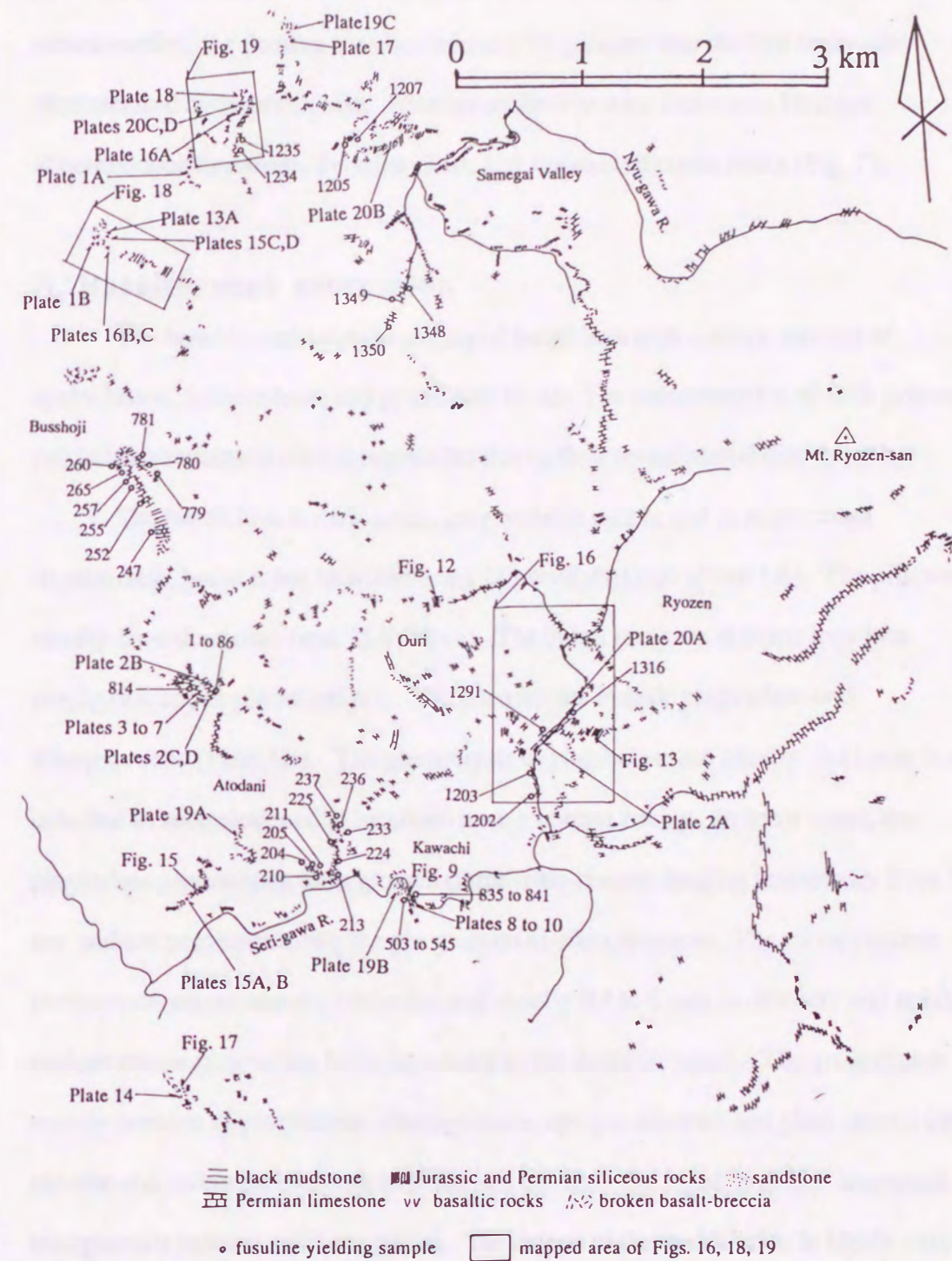


Fig. 6 Map showing the localities of outcrop-sketches and -photographs described in the thesis petrographic samples and fusuline-yielding samples.

piecing together from isolated, large-sized blocks. Through the stratigraphic reconstruction, the Suzuka oceanic rocks can be grouped into the five rock-units characterized by basaltic rocks, Permian shallow-marine limestone, Permian allochthonous limestone, Permian chert, and Jurassic siliceous rocks (Fig. 5).

A. Basaltic rock succession

The basaltic rocks consist mainly of basalt lava with a minor amount of hyaloclastite, dolerite lava, and pyroclastic rocks. The reconstruction of their primary volcanic succession is almost impossible due to their severe stratal discontinuity.

The basalt lava is dark green, gray, reddish purple and in many cases structureless, but at a few localities has a pillowed structure (Plate 1A). The pillows usually have diameters from 15 to 70 cm. The basalt lavas are at many localities porphyritic and in places aphyric. The phenocrysts include plagioclase and clinopyroxene (Plate 1B). The phenocrysts of plagioclase are usually 2-16 mm in size, euhedral to subhedral, and at localities have a normal zoning. In some cases, the plagioclase phenocrysts form glomeroporphyritic clusters ranging in diameter from 1 to 5 cm and are accompanied by the phenocrysts of clinopyroxene. The clinopyroxene phenocrysts are subhedral to anhedral and usually 0.4 to 6 mm in diameter and ophitically enclose coarse plagioclase laths, especially in the doleritic basalt. The groundmass usually consists of plagioclase, clinopyroxene, opaque minerals and glass altered into chlorite and carbonate minerals with the rare olivine. The basalt lava has intersertal and intergranular textures with amygdales. The degree of the vesiculation is highly varied. The distinct pillow-lavas are highly vesicular in many cases. The vesicles are filled with chlorite and/or calcite.

The dolerite is the coarse-grained equivalent of the basalt lava and consists

essentially of plagioclase and clinopyroxene (Plate 1C). The plagioclase occupies the most part of the dolerite, and is 0.8-1.6 in size and euhedral. The clinopyroxene is a minor component, ranging from 0.4 to 1 mm in diameter and anhedral with an ophitic texture.

Pyroclastic rocks are associated with the basalt lavas and include pyroclastic breccia, lapilli tuff, and lapillistone in terms of the classification by Fisher (1966). The pyroclastic breccia consists of fragmented pillows and breccia portions and is similar to "pillow breccia" of Staudigel and Schmincke (1984). Some blocks have a distinct pillow-structure and have intra-pillow laminations. The lapilli tuff comprises lapilli-sized basalt fragments and very fine ash-sized matrix. The fragments are angular to subrounded and comprise diverse rock-types including intersertal basalt, vesicular aphanitic basalt, and highly vesicular glass. The fragments are set in the matrix having laminae and have an indistinct preferred orientation. The lapillistone is composed mainly of fragments of tuff which contains grains of plagioclase and palagonite. The fragments of tuff are irregular and lenticular-shaped and 2 mm to 1 cm size. The matrix comprises coarse ash-sized fragments of basalt varied in lithology .

Hyaloclastites are composed of coarse ash-sized vesicular glass shards with a small amount of euhedral to subhedral plagioclases, ranging from 0.2 to 1 mm in size (Plate 1D). Most of the shards are composed of highly vesicular glasses. Shards consisting of cryptocrystalline to microcrystalline or vesicular basalts are present, but less common. These shards have been stretched and have highly irregular shapes. The vesicles are usually filled with chlorite.

B. Permian shallow-marine limestone succession

The shallow marine limestone succession consists mostly of fossiliferous limestones showing various rock-types and limestone-breccia, and is accompanied by basaltic volcanoclastics at the bottom (Fig 7). The reconstructed succession of the shallow-marine limestone succession is approximately 230 m thick and is lithologically subdivided into three members.

1. Lithostratigraphy

(1) Lower member (approximately 100 m thick)

The limestones of the lower member are dark gray to black. The dark gray limestones are structureless to thick-bedded (Plate 2A), and the black limestone is thin- to thick-bedded. The beds range in thickness from several centimeters to a few meters. The distinctly thin-bedded black limestones are carbonaceous and have black calcareous, carbonaceous matter-rich claystone partings of less than several centimeters thickness. The bedded limestones are often intraformationally folded. At the base of the succession, the dark gray limestone is thinly interbedded with dark green basaltic volcanoclastic sandstone composed of basalt detritus of silt- to sand- size. Limestone-sandstone which contains a few grains of scoria and dolomite occurs intercalated in the lower part of the lower member.

The most characteristic particles of the lower member are peloids, thick-shell bivalves, and cyanobacterias. Subordinate are the small foraminifers, gastropods, brachiopods, crinoids, fusulines, ostracods, *Tubiphytes*, green algae, red algae, echinoids, corals, and calcispheres. In addition to these organic debris, a large amount of algal peloids is contained in the matrix.

Most of the limestones of the member are described as lime-wacke/mudstone. A

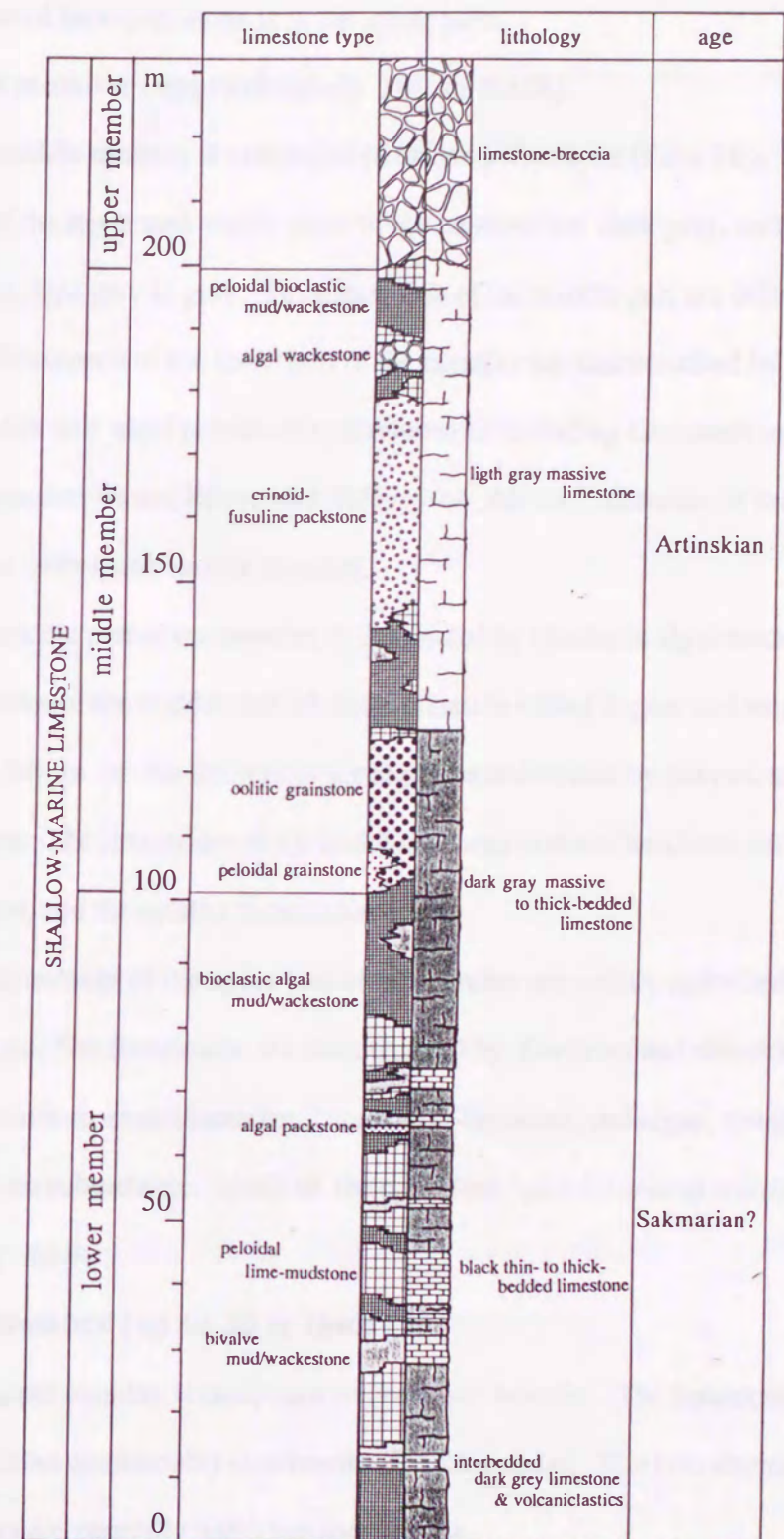


Fig. 7 Composite columnar sections showing the lithostratigraphy and age of Permian shallow-marine limestones, pieced together from several, isolated blocks.



lesser amount of lime-packstone is in the upper part.

(2) Middle member (approximately 100 m thick)

The middle member is composed of massive limestone (Plate 2B). The limestones of the lower and middle parts of the member are dark gray, and those of the upper part are light gray to gray. The limestones of the middle part are dolomitized.

The limestones of the lower part of the member are characterized by a large amount of ooids and algal peloids of cyanobacterias including *Girvanella* and the subordinate smaller foraminifers, and *Tubiphytes*. All the limestones of the lower part are grainstone with sparry calcite cements.

The middle part of the member is dominated by bioclastic algal wackestone. All of the limestones of the middle part are dolomitized to varied degree and recrystallized. The primary fabrics of the limestones are at places obliterated by intense, severe dolomitization. The limestones of the middle member contain fusulines, crinoids, cyanobacterias, and the smaller foraminifers.

The limestones of the upper part of the member are mainly described as packstone and wackestone. The limestones are characterized by fusulines and crinoids. The smaller foraminifers, cyanobacterias, *Tubiphytes*, bryozoas, red algae, bivalves, and algal peloids are subordinate. Much of the packstone has a lime-mud matrix and spar-filled primary voids.

(3) Upper member (up to 30 m thick)

The upper member is composed of limestone-breccia. The limestone-breccia of the upper member conformably overlies the middle member. The boundaries between these members are generally indistinct and uneven.

The limestone-breccia is massive and consists mainly of a large amount of limestone clasts of various rock-types and a small amount of dolomite detritus with very

rare or no lime-mudstone matrix.

The limestone clasts are unsorted, ranging in size from a few millimeters to several meters, and essentially angular-shaped. The lithoclasts are supported by one another and completely disorganized without any oriented fabrics.

2. Age

The shallow-marine limestone was dated by means of the fusuline biostratigraphy. From the bioclastic limestones of the study area, 17 fusuline species belonging to 9 genera were yielded. They are listed in Tables 1, 2, 3 with their sample numbers.

From the lower member, no fusulines available for the precise age determination were yielded. The fusulines including *Minojapanella* sp., *Pseudoschwagerina* ? sp., *Pseudofusulina* sp., and *Biwaella* sp. may indicate that the lower member is correlated to the Sakmarian.

The middle member and all the limestone clasts of the upper member are referred to as the *Pseudofusulina vulgaris* Zone indicative of the lower to middle Artinskian. *Pseudofusulina exigua* (Schellwien), *Pseudofusulina fusiformis* (Schellwien), *Pseudofusulina lutugini* (Schellwien), and *Pseudofusulina vulgaris* (Schellwien) are characteristic of the fusuline fauna. Noteworthy is that the limestone clasts yield no fusulines showing different ages from the Artinskian.

taxa \ locality	204	205	210	211	213	224	225	237	814	1202	1203	1291	1316
<i>Biwaella</i> sp.							◆?	◆?					
<i>Pseudoschwagerina</i> sp.					◆		◆?		◆			◆?	
<i>Paraschwagerina</i> sp.							◆?						
<i>Pseudofusulina</i> sp.	◆*	◆*	◆*	◆*		◆?		◆		◆*	◆		◆
<i>Schubertella</i> sp.		◆											
<i>Minojapanella</i> sp.					◆								

* : advanced form

Table 1 List of fusulines from the lower member of the shallow-marine limestone succession.

taxa	locality	1	4	5	6	7	8	9	10	11	14	15	16	43	47
<i>Biwaella</i> sp.															◆?
<i>Paraschwagerina</i> sp.														◆	◆
<i>Acervoschwagerina</i> sp.												◆			
<i>Pseudofusulina</i> sp.		◆	◆*												
<i>P. ambigua</i> (DEPRAT)					◆'										
<i>P. fusiformis</i> (SCHELLWIEN)						◆		◆'	◆'	◆			◆'		
<i>P. krafftii</i> (SCHELLWIEN)							◆								
<i>P. lutugini</i> (SCHELLWIEN)				◆							◆*				◆'
<i>P. tschernyschewi</i> (SCHELLWIEN)					◆'										
<i>Schubertella</i> sp.								◆	◆	◆					

taxa	locality	51	52	56	59	62	63	64	70	71	72	73	86	233	236
<i>Biwaella</i> sp.															◆?
<i>Paraschwagerina</i> sp.						◆							◆	◆	◆
<i>Pseudofusulina</i> sp.			◆*	◆*	◆*			◆*	◆*						
<i>P. fusiformis</i> (SCHELLWIEN)											◆				
<i>P. lutugini</i> (SCHELLWIEN)		◆'							◆'					◆'	

taxa	locality	247	779	780	781	1205	1207	1234	1235	1348	1349	1350
<i>Biwaella</i> sp.						◆?	◆					
<i>Pseudoschwagerina</i> sp.								◆?				
<i>Paraschwagerina</i> sp.				◆								
<i>Pseudofusulina</i> sp.						◆						
<i>P. exigua</i> (SCHELLWIEN)					◆'							
<i>P. kueichihensis</i> (CHEN)											◆'	
<i>P. tschernyschewi</i> (SCHELLWIEN)								◆'				
<i>P. vulgaris</i> (SCHELLWIEN)		◆'	◆'									◆
<i>Schubertella</i> sp.							◆				◆	◆

* : advanced form, " : confer, ' : ex. gr.

Table 2 List of fusulines from the middle member of the shallow-marine limestone succession.

taxa	locality	17	19	20	21	23	24	25	26	27	30	36a	36b	75	252	255	257	260	265	
<i>Biwaella</i> sp.							◆?				◆									
<i>Schwagerina</i> sp.																				
<i>S. krotowi</i> (SCHELLWIEN)												◆'								
<i>Pseudoschwagerina</i> sp.		◆																		
<i>Paraschwagerina</i> sp.			◆?											◆		◆?				
<i>Pseudofusulina</i> sp.			◆?														◆	◆	◆	◆?
<i>P. lutugini</i> (SCHELLWIEN)							◆'				◆*									
<i>P. tschernyschewi</i> (SCHELLWIEN)				◆'																
<i>P. vulgaris</i> (SCHELLWIEN)					◆'	◆	◆*		◆	◆	◆'									
<i>P. globosa</i> (SCHELLWIEN)								◆'												
<i>Schubertella</i> sp.				◆		◆	◆		◆		◆									◆
<i>Mesoschubertella</i> sp.													◆?							
<i>Nankinella</i> sp.											◆									

" : confer, ' : ex. gr.

Table 3 List of fusulines from the limestone-breccia.

Unit	Thickness (m)	Color	Texture	Fabric	Dominant Grain Type	Remarks
1	1.5	Light grey	Massive	peloidal	lime-mudstone	
2	1.5	Light grey	Massive	bivalve	lime-mud/wackestone	
3	1.5	Light grey	Massive	bioclastic	lime-mud/wackestone	
4	1.5	Light grey	Massive	peloidal	lime-grainstone	
5	1.5	Light grey	Massive	oolitic	lime-grainstone	
6	1.5	Light grey	Massive	crinoid-fusuline	lime-wacke/packstone	
7	1.5	Light grey	Massive	algal	lime-wackestone	
8	1.5	Light grey	Massive	limestone-breccia		

Unit	Thickness (m)	Color	Texture	Fabric	Dominant Grain Type	Remarks
1	1.5	Light grey	Massive	peloidal	lime-mudstone	
2	1.5	Light grey	Massive	bivalve	lime-mud/wackestone	
3	1.5	Light grey	Massive	bioclastic	lime-mud/wackestone	
4	1.5	Light grey	Massive	peloidal	lime-grainstone	
5	1.5	Light grey	Massive	oolitic	lime-grainstone	
6	1.5	Light grey	Massive	crinoid-fusuline	lime-wacke/packstone	
7	1.5	Light grey	Massive	algal	lime-wackestone	
8	1.5	Light grey	Massive	limestone-breccia		

3. Limestone-types

The limestone-types of the shallow-marine limestone are grouped into eight major types with fabrics and dominant grain-types: (1) peloidal lime-mudstone, (2) bivalve lime-mud/wackestone, (3) bioclastic lime-mud/wackestone, (4) peloidal lime-grainstone, (5) oolitic lime-grainstone, (6) crinoid-fusuline lime-wacke/packstone, (7) algal lime-wackestone, (8) limestone-breccia. The minor varieties occur, including algal lime-packstone in the lower member, which contains abundant algal oncoids formed by encrustation of cyanobacterias.

(1) Peloidal lime-mudstone

The limestone of this type is characterized by dominance of the well-sorted peloidal lime-mud matrix and scarcity of coarse skeletal debris (Plate 3A). A small amount of bivalves, gastropods, brachiopods, ostracods, crinoids, calcispheres, and cyanobacterias is in places scattered. All these skeletal debris are supported by the matrix.

This type of limestone is common in the lower member and is found also in the middle member.

(2) Bivalve lime-mud/wackestone

The limestone of this type consists of abundant thick- and thin-shelled bivalves (Plate 3B) and their fragments with a small amount of green algae, cyanobacterias, ostracods, crinoids, calcispheres, the smaller foraminifers, *Tubiphytes*, gastropods, and brachiopods. All the skeletal particles are supported by the matrix is composed of a mixture of lime-mud and silt-sized bioclastic grains. Bivalve shells and crinoid oscicles are in places encrusted by cyanobacterias.

This type is common in the lower member and is found also in the middle member. Some of limestone clasts of the upper member comprise this type of limestone.

(3) Bioclastic lime-mud/wackestone

The limestone of this type contains diverse skeletal debris, including the smaller foraminifers, calcispheres, bivalves, gastropods, brachiopods, echinoids, ostracods, crinoids, fusulines, cyanobacterias, red algae, *Tubiphytes obscurus* Masolv, and algal oncoids (Plates 3C, 4A). These organic debris are supported by the poorly sorted lime-mud matrix with silt- to sand-sized bioclasts and peloids.

The cyanobacterias and *Tubiphytes* occur as algal tissues covering skeletal particles and micritic layers of oncoids. Algal-encrusted bioclastic particles are often micritized. Red algae are characterized by the reticulate structure formed by thin micrite walls separating small cells and the holes filled with sparite (Plates 3C, D).

The limestone of this type is common in the lower and middle members and also occurs as the lithoclasts in the limestone-breccia of the upper member.

(4) Peloidal lime-grainstone

Characteristic of this type is a considerable amount of peloids contained together with a small amount of bioclasts (Plates 4B). Skeletal debris include cyanobacterias, crinoids, calcispheres, the smaller foraminifers, and *Tubiphytes*. The peloids are very well sorted and medium sand-sized. Most of them are algal peloids originated from girvanellid cyanobacterias. All skeletal grains is filled by sparry calcite cement.

The limestone of this type is limited to the bottom of the middle member.

(5) Oolitic lime-grainstone

Most of grains of this type comprise ooids (Plate 4C). Fragments of crinoids and bivalves with a small amount of fusulines and ostracods are identified as nuclei of ooids. The ooids are well sorted, 0.8 to 1.0 mm in diameter and have regular concentric micritic laminae coating a nucleus. The ooids are supported by each other and cemented by the spar.

The oolitic lime-grainstone occurs restricted in the lower part of the middle member.

(6) Algae-crinoid-fusuline lime-wacke/packstone

Essential skeletal debris of this type are fusulines and crinoids (Plates 5A, C). A large amount of minute tubes, which is supposed to be calcareous algae, are contained (Plate 5D). Associated with these biogenic particles, a small amount of cyanobacterias, red algae including *Parachactetes* (Plate 5B), green algae, the smaller foraminifers, *Tubiphytes obscurus* Masolv, and brachiopods are contained. The crinoids and brachiopod shells are encrusted and micritized by cyanobacterias. All the skeletal grains are densely packed and supported by one another (Plates 5A) and are in places randomly embedded in and supported by a matrix (Plates 5). The matrix is composed of poorly sorted lime-mud with some fine-grained bioclasts.

The limestone of this type is common in the middle member and occurs as lithoclasts of limestone-breccia of the upper member.

(7) Algal lime-wackestone

Accompanied by a small amount of fusulines, the smaller foraminifers, crinoids, *Tubiphytes*, calcispheres, ostracods, bivalves, and gastropods, short, tube-shaped cyanobacterias are the essential skeletal component of this type (Plate 6A). Cyanobacterias also occur as algal envelopes (Plate 6B). Most of the skeletal debris are supported by a lime-mud matrix and partly cemented by sparite.

The limestone of this type is in the upper part of the middle member and occurs as lithoclasts of limestone-breccia in upper member.

(8) Limestone-breccia

The limestone-breccia contains abundant limestone clasts with a small amount of dolomite detritus and skeletal debris (Plate 2C). The limestone clasts are varying in size

from a few millimeters to several meters, and angular-shaped. The rock-types of the limestone clasts are dominated by fusuline-crinoid lime-packstone and fusuline-peloidal lime-grainstone and include subordinate bioclastic lime-wackestone and algal bindstone. Almost all the limestone clasts are closely similar to the shallow-marine limestones of the middle member except for fusuline-peloidal lime-grainstone and algal bindstone.

Fusuline-peloidal lime-grainstone clast is characterized by abundant peloidal particles and fusulines (Plate 6C, D). Subordinate are the smaller foraminifers, cyanobacterias, green algae including *Gyroporella* and *Pseudogyroporella*, bivalves, gastropods, and crinoids. Most of fusulines and crinoids are coated by thin algal micrite (Plate 6D). The type locally contains a small amount of intraclasts composed of lime-mudstone. All these particles are supported by one other and cemented by the sparite. Algal bindstone clast comprises thinly laminated layers of cyanobacterias and *Archaeodispoleum* with primary open spaces (Plates 8A, B, C). A large amount of skeletal debris including fusulines, the smaller foraminifers, bivalves, gastropods, calcispheres, *Tubiphytes*, and green algae is embedded within the algal layers. The open spaces within the algal mats are filled by sparry calcite.

The matrix of the limestone-breccia is composed of well sorted lime-mud and mixture of lime-mud/silt and fine-grained bioclastic debris including fusulines, crinoids and algae. The lime-mud matrix also contains dolomite detritus, which are well-sorted, anhedral, and medium sand-sized. In case that the matrix is absent, the lithoclasts are in stylolitic-sutured contact with one another (Plate 2D).

The limestone-breccia occurs only in the upper member of the shallow-marine limestone succession.

C. Permian allochthonous limestone succession

The allochthonous limestone succession is characterized by redeposited shallow-marine limestone of various rock-types with a great admixture of reworked basaltic debris of diverse grain sizes (Fig. 8). All the constituents of the succession show reworked natures, but no contamination of distinct land-derived clastic materials was identified in the field and under the microscope.

The primary stratigraphy was reconstructed, pieced together from outcrops in a few of isolated blocks. The reconstructed succession attains up to 17 m thick and is lithologically divided into the lower and upper members.

1. Lithostratigraphy

(1) Lower member

The lower member comprises an orderly succession chiefly of well stratified reworked sediments comprising lime-mudstone, lime-packstone, limestone-sandstone with a few intercalations of volcanoclastic mudstone, limestone-basalt-conglomerate (Fig. 10) and talus blocks of limestone (Fig. 8). The thickness of the member, so far as exposed, reaches 9 m or more.

Most of the constituent rocks show a well defined stratification. Each of beds ranges in thickness from a few centimeters to 1 meter. A few kinds of internal sedimentary structures due to currents and flows are seen in the beds.

The reworked lime-mudstone (Plates 8A, 9A) consists of sorted lime-silt and mud which contain a small amount of skeletal debris smaller than the sand size. The skeletal debris are often fragmented and abraded and comprise fusulines and crinoids. Coarse sand- to granule-sized fragments of basaltic rocks and silt-sized plagioclase debris are

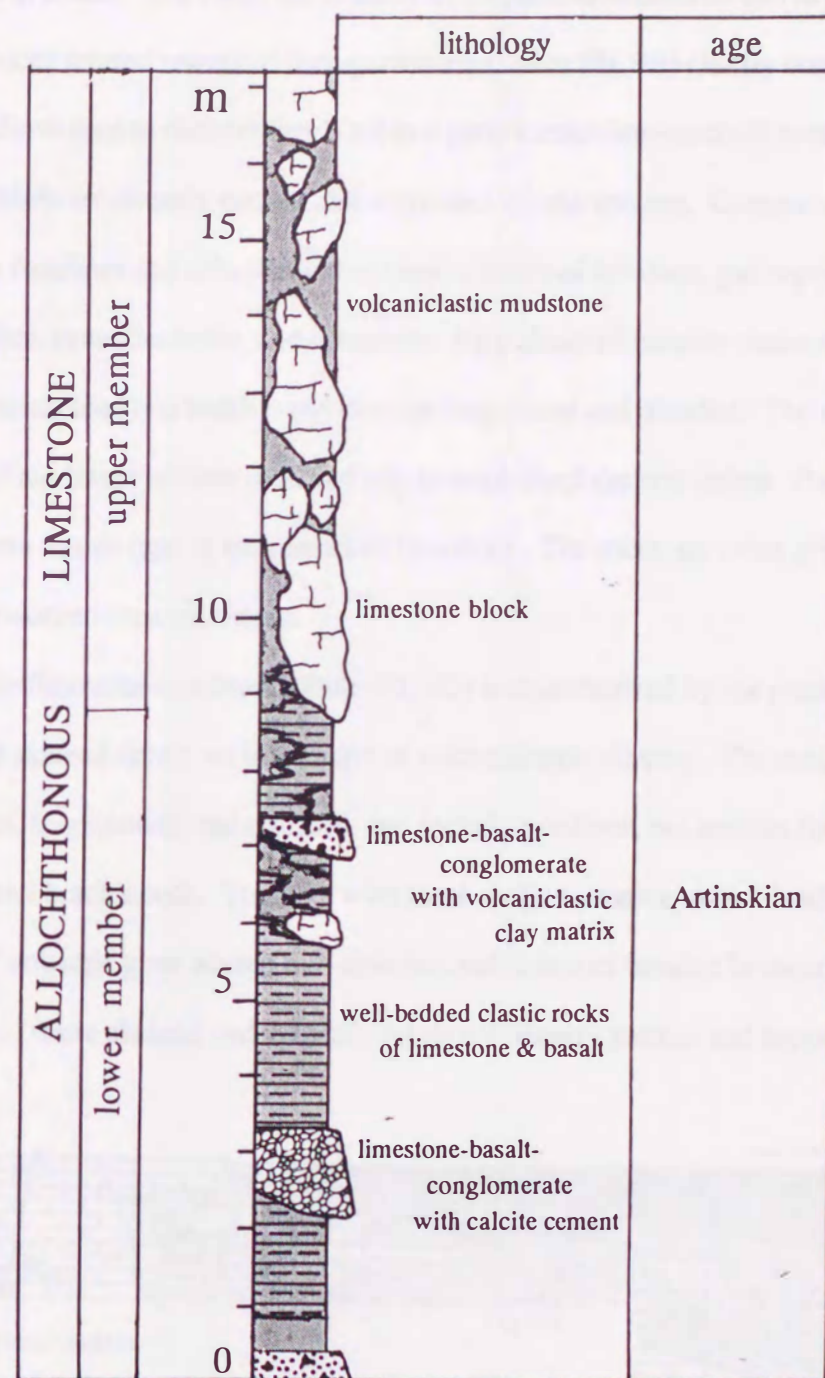


Fig. 8 Generalized columnar section showing the lithostratigraphy and age of Permian allochthonous limestones pieced together from several isolated blocks.



contained in places. The rocks are in many cases parallel-laminated and in places graded.

Rocks termed reworked lime-packstone (Plates 8B, 9B) chiefly comprise sand-sized, shallow-marine skeletal debris set in a poor-sorted lime-mud/silt matrix. The skeletal debris are densely packed and supported by one another. Common skeletal debris are fusulines and crinoids with a small amount of bivalves, gastropods, the smaller foraminifers, cyanobacterias, and ostracods. Rare clasts of basaltic rocks are present. All of these skeletal and basaltic particles are fragmental and abraded. The matrix consists of a mixture of lime-mud and silt- to sand-sized skeletal debris. Parallel laminae are common in this type of the reworked limestone. The rocks are often graded upward into the reworked lime-mudstone.

The limestone-sandstone (Plate 8D, 9D) is characterized by the predominance of sand-sized skeletal debris set in a matrix of volcanoclastic silt/clay. The skeletal debris are well sorted, fragmentary and rounded, and include fusulines, the smaller foraminifers, crinoids, and brachiopods. Together with these shallow-marine skeletal debris a small amount of volcanic glass altered into chlorites and debris of basaltic lavas are scattered in the matrix. These skeletal and volcanic debris are densely packed and supported by one

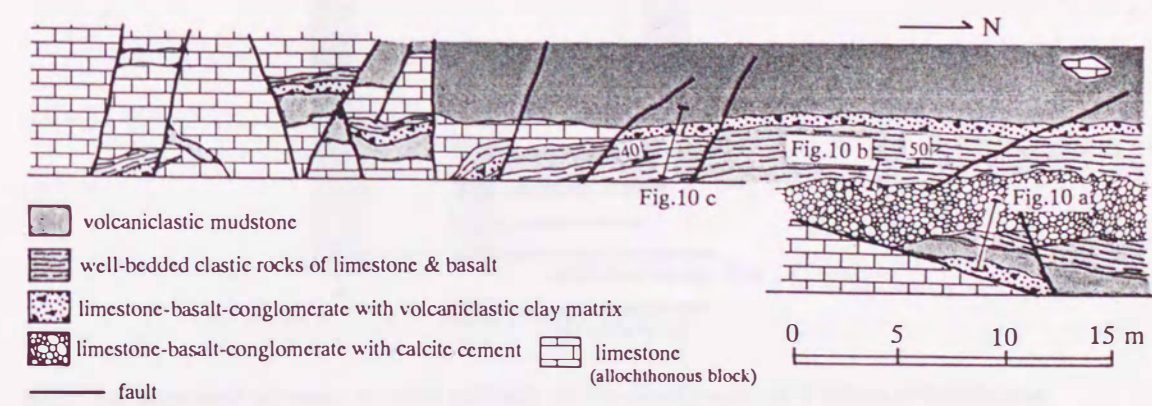


Fig. 9 Outcrop sketch showing the occurrence of well-bedded reworked limestones and allochthonous blocks of shallow-marine limestone. Locality is shown in Fig. 6.

The Permian allochthonous limestone is characterized by a complex lithostratigraphy. The sequence is dominated by volcaniclastic mudstone, which is interbedded with various types of limestone. These include reworked lime-mud/packstone, limestone-sandstone, and limestone-basalt-conglomerate. The conglomerate units are further distinguished by their matrix: some have a volcaniclastic clay matrix, while others are cemented with calcite. The thickness of these units varies significantly, with some reaching up to 2 meters. The overall structure is highly irregular, reflecting the allochthonous nature of the deposit.

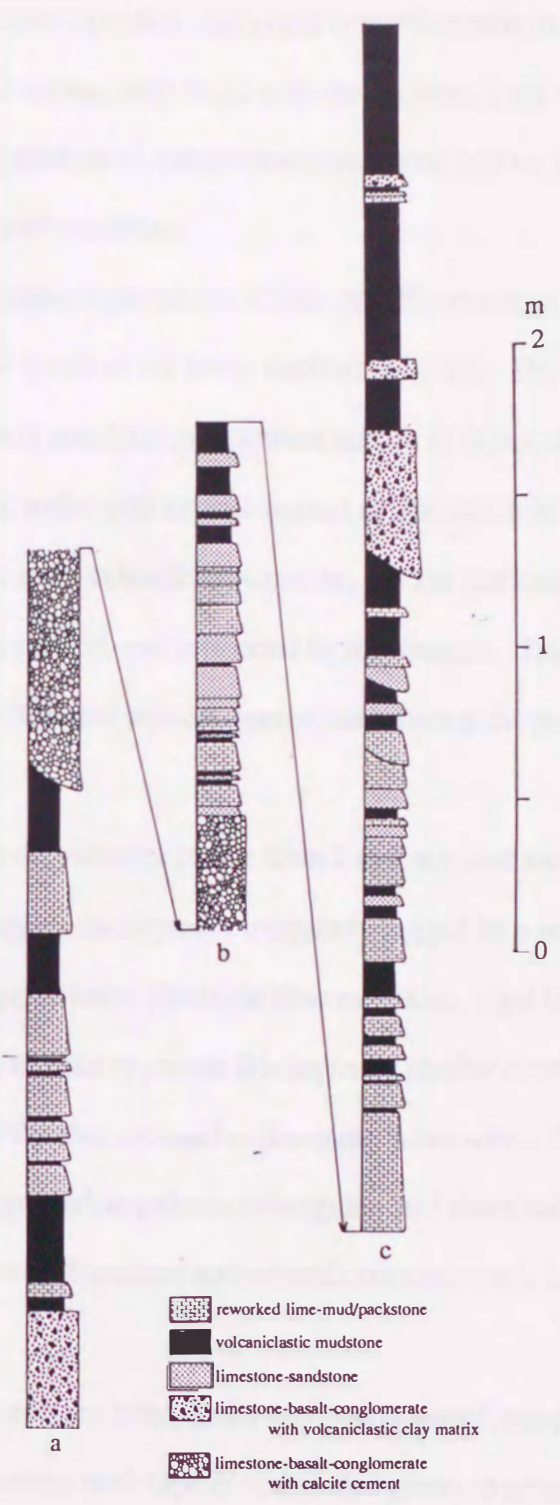
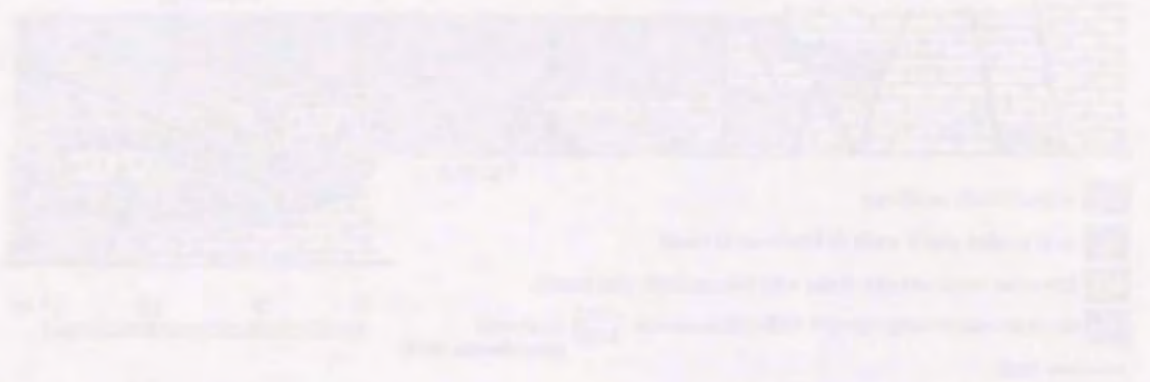


Fig. 10 Measured columnar sections showing the lithostratigraphy of Permian allochthonous limestone. See Fig. 9 for localities.

another. The intense stylolitization along their contacts results in severe recrystallization.

Limestone-sandstone beds range in thickness from 1 cm to 50 cm. The beds often contain parallel laminae of volcanoclastic mudstone and are graded into an overlying laminae of volcanoclastic mudstone.

Limestone-basalt-conglomerate (Plates 10A, B) occurs as intermittent intercalations at a few levels of the lower member (Fig. 10). The beds reach up to 1 m thick. Limestone-basalt conglomerate consists mainly of debris of shallow-marine limestone and basaltic rocks with a small amount of isolated individuals of shallow-marine calcitic fossils and a volcanoclastic matrix. All the particles are unoriented, disorganized, densely packed, and supported by one another. The calcareous particles are often stylolitized. The rare primary open-spaces among the particles are filled by spary calcite.

The limestone debris range in size from 1 to 3 mm and are often subrounded to subangular. Their margins are in places irregularly rugged by a strong stylolitization. The common clast-type includes bioclastic lime-mudstone, algal bindstone, and crinoid-fusuline grainstone. The clast-types are lithologically similar closely to the rock-types of the middle member of the shallow-marine limestone succession. The isolated skeletal debris are mostly fragmented, angular to subangular, and chaotically scattered together with the limestone debris. Fusulines and crinoids are commonly found as the isolated skeletal debris.

The basaltic debris are subrounded and poorly sorted, ranging in size from 0.5 mm to 5 mm. The common rock-type is vesiculated glassy to aphanitic basalt lava, and intersertal basalt and glomeroporphyritic basalt are subordinate.

Volcanoclastic mudstone is dark gray to black and mainly comprises volcanoclastic clay containing abundant silt-sized bioclastic debris of coarse silt- to very

fine-sized and angular plagioclases (Plates 8C, 9C). Volcaniclastic mudstone commonly contains skeletal debris including fusulines, crinoids, ostracods, and brachiopods (Plate 9C). The skeletal debris are angular to subangular in shape. The skeletal debris at many localities are randomly scattered in a volcaniclastic matrix, but are crudely oriented in places where a volcaniclastic mudstone has a graded structure.

(2) Upper member

The upper member, up to 8 m thick, is characterized by limestone talus blocks chaotically embedded in a matrix of volcaniclastic mudstone with coarser-grained reworked limestone. The limestone blocks are usually irregular-shaped, unsorted, ranging in size from a few meters to approximately ten meters or more, and completely disorganized. The limestone-types of the blocks include fusuline lime-mud/wackestone, fusuline lime-grainstone, and limestone-breccia and are lithologically similar to the components of the middle and upper members of the shallow-marine limestone succession. The blocks of the limestones yielded no fusulines available for the precise age determination, except for *Paraschwagerina* sp., *Biwaella* sp., *Pseudofusulina* sp., and *Schubertella* sp. (Table 4).

The limestone blocks in many cases occur crowded to form a dense-packed aggregate and are supported by one another. In places, however, the blocks are isolated and chaotically embedded within the well-bedded reworked limestones (Fig. 9). The limestone blocks have lithologically sharp boundaries to the surrounding sediments. The stratification of the underlying reworked limestone has been often disturbed and cut by the limestone blocks. Fusuline debris embedded in the underlying the limestone blocks are squashed owing to the loading of the limestone blocks.

2. Age

The redeposited limestone was dated by means of the fusuline biostratigraphy

taxa \ locality	503	504	505	511	514	515	517	519	520	522	523	524	528
<i>Biwaella</i> sp.					◆?	◆?							
<i>Paraschwagerina</i> sp.				◆					◆				◆?
<i>Acervoschwagerina</i> sp.													
<i>A. endoi</i> HANZAWA	◆	◆	◆					◆	◆	◆	◆	◆	◆
<i>Pseudofusulina</i> sp.					◆?								
<i>Schubertella</i> sp.			◆		◆	◆				◆			

taxa \ locality	530	536	537	541	543	544	545	835	836	837	838	839	841
<i>Biwaella</i> sp.		◆?	◆?									◆?	
<i>Paraschwagerina</i> sp.									◆		◆		◆?
<i>Acervoschwagerina</i> sp.	◆			◆			◆		◆				
<i>A. endoi</i> HANZAWA					◆								
<i>Pseudofusulina</i> sp.						◆					◆		
<i>P. vulgaris</i> (SCHELLWIEN)												◆	◆
<i>Schubertella</i> sp.	◆	◆	◆			◆	◆		◆			◆	◆

* : advanced form, ' : ex. gr.

Table 4 List of fusulines from blocks in the allochthonous limestone succession .

taxa \ locality	512	513	540	840
<i>Biwaella</i> sp.		◆		
<i>Paraschwagerina</i> sp.	◆?	◆		◆
<i>Pseudofusulina</i> sp.			◆	
<i>Schubertella</i> sp.		◆	◆	

Table 5 List of fusulines from well-bedded clastic rocks in the allochthonous limestone succession.

(Table 5) . The examined fusulines were detected from clastic limestone beds.

In spite of the fact that fusulines embedded in the clastic limestone beds were actually reworked, *Acervoschwagerina endoi* Hanzawa and *Pseudofusulina vulgaris* (Schellwien) are indicative of the approximate age of their accumulation. Microscopic examination reveals that chambers of these fusulines have been filled with undeformed spars after the disruption of walls and septa by loading of the overlying limestone talus blocks. In other words, the fusulines were crushed immediately after their re-sedimentation. Thus, the primary sedimentation of the redeposited limestone could be best dated by these fusulines, though reworked.

All lines of paleontological and petrographic evidence reveal that the redeposited

Unit	Thickness (m)	Color	Bedding	Fossils
1	0-10	Dark gray	Bedded	None
2	10-20	Dark gray	Structureless	None
3	20-30	Dark gray	Interbedded	None
4	30-40	Dark gray	Acidic tuff	None
5	40-50	Dark gray	Siliceous shale	None

Unit	Thickness (m)	Color	Bedding	Fossils
6	0-5	Dark gray	Bedded	None
7	5-10	Dark gray	Structureless	None
8	10-15	Dark gray	Interbedded	None
9	15-20	Dark gray	Acidic tuff	None
10	20-25	Dark gray	Siliceous shale	None

limestone is referred to as the *Pseudofusulina vulgaris* Zone, indicative of the lower to middle Artinskian age. Therefore, the redeposited limestone is time-equivalent with the middle member of the reconstructed succession of the shallow-marine limestone.

D. Permian chert succession

1. Lithology

This succession consists almost entirely of ribbon chert with a small amount of dolomite. The thickness of the succession attains up to 50 m.

Chert is red or bluish-gray and thinly bedded with siliceous claystone partings. Each of chert beds is several centimeters in thickness and claystone partings are less than a few millimeters. The chert contains radiolarians and siliceous sponge spicules and locally has intercalations of dolomite-sandstone. The beds of dolomite-sandstone range in thickness from several to a few tens centimeters. Dolomite-sandstone comprises anhedral grains of dolomite and has an arenitic texture with very rare or no matrix.

2. Age

No datable radiolarian fossils have been obtained from the chert. However, Suetsugu (1981MS) reported upper Lower Permian conodonts including *Sweetgnathus* cf. *S. whitei* (Rhodes) from the chert.

E. Jurassic siliceous rock succession

1. Lithostratigraphy

The Jurassic siliceous rock succession begins with bedded chert, followed by structureless chert, and succeeded by interbedded chert and acidic tuff, which is, in turn, overlain by siliceous shale (Fig. 11). The structureless chert contains laterally discrete, lenticular intercalations of conglomerate of Jurassic deep-water limestone (Fig. 12) and blocks of Permian shallow-water limestone (Fig.13).

The bedded chert section is up to 4 m in thickness. The cherts are dark-gray and

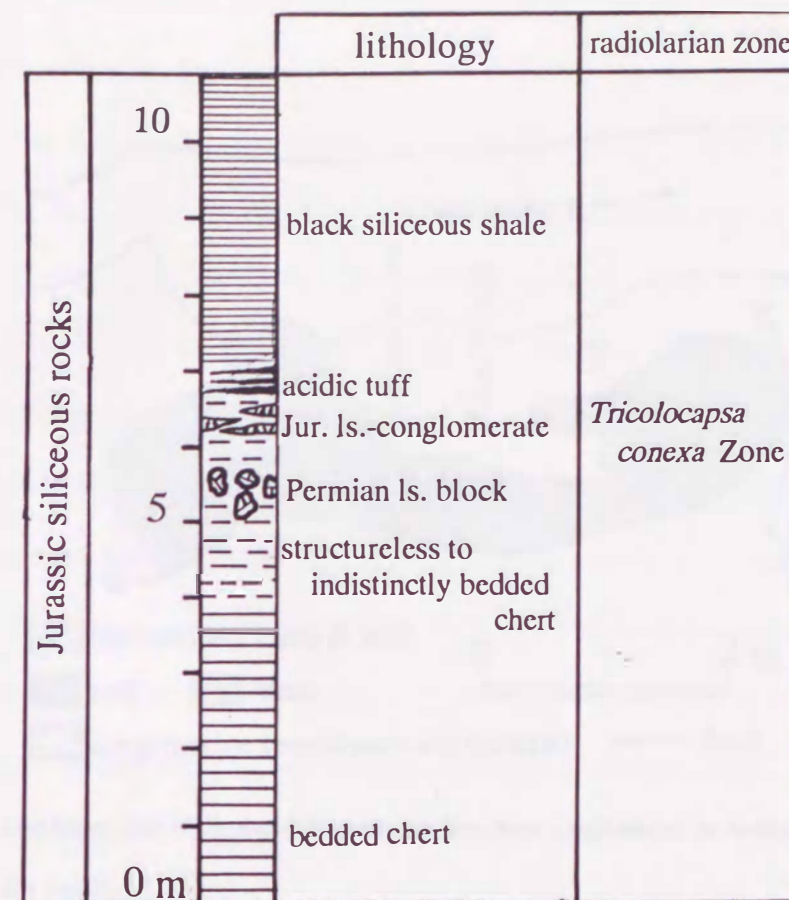


Fig. 11 Generalized columnar section showing the lithostratigraphy and radiolarian zone of Jurassic siliceous rocks.

have the rare partings of siliceous claystone. Individual chert beds are commonly several centimeters thick. The chert yields radiolarian fossils.

The structureless chert which has faint vestiges of clayey partings is approximately 4 m thick and dark gray to pale-greenish gray. Although the chert is more muddy than the bedded variety of chert, no terrigenous detritus coarser than the silt-size was identified. Manganese carbonate occurs forming thin veins and micro-nodules ranging in diameter from 0.04 to 0.06 mm in the chert. Chalcedonic quartz of radiolarian fossils is often replaced by the manganese carbonate.

The deep-water limestone conglomerate contains abundant limestone clasts with

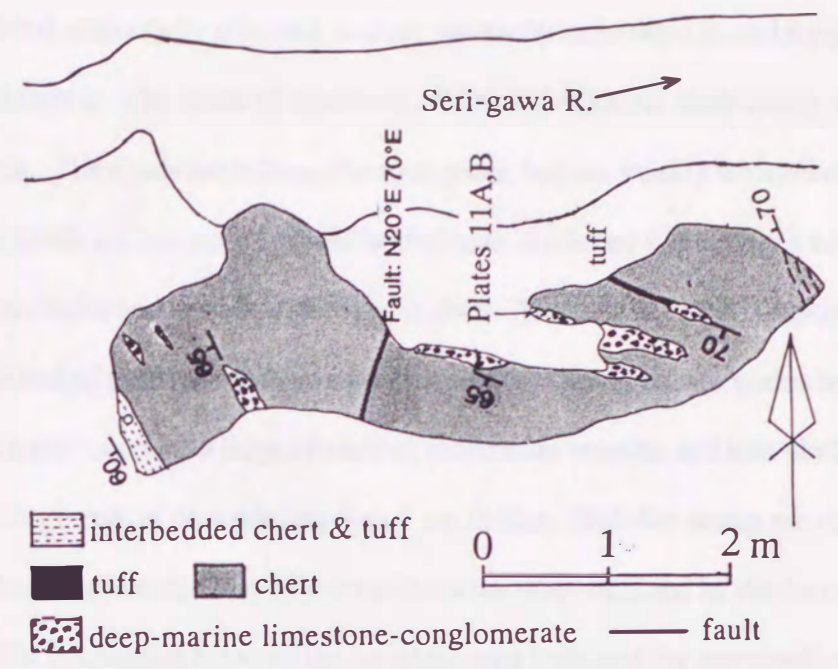


Fig. 12 Lenticular beds of displaced deep-marine limestone conglomerate in Jurassic radiolarian chert. See Fig. 6 for locality.

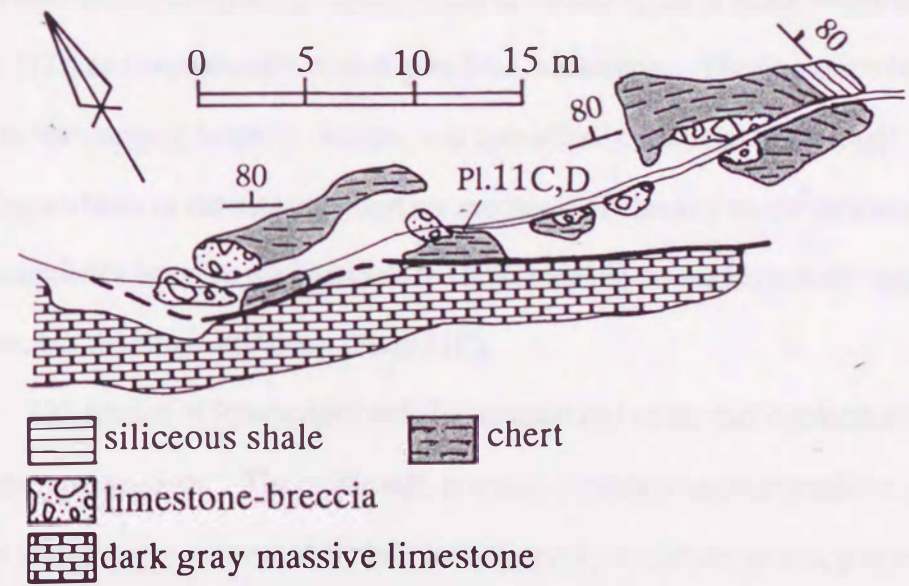


Fig. 13 Displaced Permian limestone-breccia in Jurassic chert. Locality in Fig. 6.



a small amounts of clasts of chert and siliceous shale (Plates 11A, B). All the clasts are poorly sorted, chaotically oriented, and are randomly embedded in and supported by lime-mud matrix. The clasts of limestone, chert, and siliceous shale rarely exceed 3 cm in diameter. The clasts are subangular to angular, but are weakly water-worn. The limestone clasts are composed of well sorted lime-mudstone containing a large amount of radiolarian fossils and very thin-shelled bivalves. The matrix of the conglomerate is gray and composed of poorly sorted, coarser lime-silt containing calcite grains less than 1mm. The matrix also contains a large amount of radiolarian remains and thin-shelled bivalves with rare fragments of crinoids less than 1 cm in size. Stylolite seams are commonly discernible in the matrix. The limestone clasts are often outlined by distinct stylolite seams. The boundaries between the conglomerate beds and the surrounding chert are lithologically sharp.

The limestone blocks embedded in structureless chert are composed mainly of limestone-breccia comprising angular clasts of various types of shallow-marine limestone (Plate 11D) and occasionally of dark gray lime-wackestone. The limestone blocks are pod- or slab-shaped, laterally discrete, and sporadically scattered in the chert. The crude bedding surfaces of the massive chert are mechanically broken by the limestone blocks. The boundaries between the chert and the limestone blocks are irregularly rugged and uneven, but lithologically sharp (Plate 11C).

The section of interbedded radiolarian chert and acidic tuff conformably overlies the structureless chert. The acidic tuff contains crystals of monocrystalline quartz and biotite with a minor amount of crystals including polycrystalline quartz, plagioclase, and K-feldspar. The crystals range in size from 0.05 to 0.2 mm. Some grains of quartz are well rounded. Chert fragments, 0.1 to 0.2 mm in size, and radiolarian fossils are in places scattered in acidic tuff.

The chert becomes more argillaceous up-section and grades into siliceous shale. The siliceous shale is black and shows no distinct sedimentary structures. The siliceous shale section is up to 4 m in thickness. The siliceous shale yields a large amount of radiolarian fossils and contains no coarse terrigenous detritus.

2. Age

(1) Siliceous rocks

Yamagata (1992) has reported the datable Jurassic radiolarian fossils from bedded chert, structureless chert, acidic tuff, and siliceous shale. All these siliceous rocks yield *Eucyrtidiellum* sp. cf. *E. unumaense* Yao, which indicates Middle to early Late Jurassic in age. The radiolarian dating reveals that the structureless chert section belongs to the Callovian to Oxfordian *Tricolocapsa conexa* Assemblage (Matsuoka, 1983), in which *Tricolocapsa conexa* Matsuoka, *T. plicarum* Yao, *Eucyrtidiellum* sp. cf. *E. unumaense* Yao are characteristic.

(2) Deep-water limestone conglomerate

Radiolarian fossils available for age determination have been obtained from the lime-mud matrix of the deep-water limestone conglomerate (Yamagata, 1992). The matrix yields *Eucyrtidiellum* sp. cf. *E. unumaense* Yao, indicative of the Middle to early Late Jurassic. The deep-water limestone conglomerate is referable to the Middle to early Late Jurassic and considered to be time-equivalent with the surrounding chert.

V. Internal textural destruction of Suzuka oceanic rocks and their chaotic intermixing

As illustrated in the geologic map (Fig.3), the Suzuka unit comprises a compositionally heterogeneous aggregate of oceanic-rock masses chiefly of Permian age

and subordinately of Jurassic age. The oceanic-rock masses notably vary in size from a few millimeters to a few kilometers. The masses are completely chaotically set in a matrix of brecciated basaltic rocks, herein termed broken basalt-breccia. The careful microscopic observation revealed that the internal, mechanical, textural fragmentation fabrics are penetrative and pervasive in the masses of basaltic rocks. Their internal fragmentation is considered to have resulted from the collisional collapse of a seamount. Thus, the microscopic characteristics of the internal fragmentation are described herein in detail.

Characterization of the internal destruction fabrics of the basaltic rocks suggests a close similarity to that of the Permian and Carboniferous reefal limestone of the Akiyoshi Limestone Group described by Sano and Kanmera (1991a). Sano and Kanmera (1991a) defined *brecciation*, *comminution*, and *pulverization* as mechanical fragmentation processes which created destruction products of limestone having various sizes in the broken limestone, and classified the destruction products by their size under the microscope; brecciated rock-pieces and skeletal fragments larger than 2mm, comminuted particles from 2 mm to 1/16 mm, and pulverized particles smaller than 1/16 mm. In this paper, the terminology for the destruction processes and their products follows that proposed by Sano and Kanmera (1991a).

A. Internal textural destruction of basaltic rocks

The destruction products of basaltic rocks megascopically appear to be closely similar to dark gray to pale-green mudstone (Plate 19C). Due to the close similarity in appearance, destruction products have been described as weathered basaltic rocks comprising lavas and tuffs (i.e., Miyamura *et al.*, 1976). However, the careful

microscopic examination reveals that the internal textural destruction of their primary fabrics are widespread in the blocks of basaltic rocks including basalt lava with dolerite, hyaloclastite and pyroclastic rocks.

The destruction fabrics of the basaltic rocks are characterized by mechanical, brittle, and *in site* fragmentation of their primary textures into various-sized rock-pieces, particles, and even pasted materials and have no sedimentary structure including laminae and grading. The internal destruction in basaltic rocks is by no means related to any faults. The internal destruction fabric has no fluxion structure showing shear displacements nor polygonization and the distribution of destruction products is uneven even in one thin section (Plate 13A).

The internal destruction fabric of basaltic rocks is mostly in a brittle manner. No deformation including contortion, shortening, and flattening in a ductile manner was observed. Local ductile deformations are present, represented by a flow structure in a strongly pulverized basaltic rocks.

The difference in rock-types of parent rocks may have resulted in the difference in size of fragmented materials and degree of fragmentation. For example, when the parent basalt lava which comprises laths of plagioclase and groundmass of glass has been destructed, the glass is pulverized into a clay-sized paste, and the laths of plagioclase are comminuted and pulverized into sand- to silt-sized, angular to subangular chips (Plate 13B). In case of hyaloclastite, the destruction part consists only of clay-sized paste. It is noted that all the destruction products have no contamination of exotic rock-pieces.

The parent rock is in many places separated into several rock-pieces by the continuous destructed parts (Plate 12B). Lithology of the rock-pieces is influenced by that of the parent rock. In case of the parent rocks of basalt and dolerite lava, the rock-pieces are homogeneous (Plate 12B). The rock-pieces are highly irregular shaped and

various-sized, but the parent rock of them in some cases can be reconstructed (Plate 12B). The rock-pieces are disorganized and chaotically embedded in the destruction products without any sedimentary and tectonic structures (Plate 12A).

To be discussed is the discrimination of the destruction fabrics from primary fragmentation fabrics of lava. Most prevailing primary fragmentation of lava without contamination of exotic blocks includes autobrecciation, chill-shatter fragmentation, and explosion fragmentation. The autobreccia is monolithologic and dominated by angular breccia portions mostly without fine-grained matrix (Staudigel and Schmincke, 1984; Carlisle, 1963). The chill-shatter fragmentation is caused by thermal stress as quenching during rapid heat loss from the magma in the contact zone with cold water, and the explosion fragmentation is related in local explosive activity as trapped in hot magma is superheated and expands rapidly (Cas and Wright, 1987). Both of the fragmentation produced very angular, various-sized, and dense-packed volcaniclastic products which in places have a mortar-structure. Their features are similar to those of weak to moderate destruction fabrics. In all these fragmentation processes, however, the fragments of lava are usually glassy to aphanitic along their peripheries due to rapid cooling of magma, while the destruction products of basaltic rocks except for pyroclastic rocks and hyaloclastite contain no basalt fragments having chill-margins. Moreover, these fragmentation processes accompany no brittle destruction of crystals in basalt blocks.

The Suzuka unit contains basaltic volcaniclastic rocks including volcaniclastic mudstone and limestone-basalt conglomerate dominated by basalt clasts. These volcaniclastic rocks comprise basaltic-rocks clasts of various rock-types and contain exotic clasts of limestone and isolated calcareous fossils, and locally the clasts are cemented by sparry calcite. Much of the volcaniclastic rocks has sedimentary structures including bedding, laminae, and grading. These features distinguish basaltic

volcaniclastic rocks from destruction products of basalt.

The destruction fabric in pyroclastic rocks and hyaloclastite is recognized by the destruction parts oblique to their primary textures. However, in case of very strongly crushed pyroclastic rocks and hyaloclastite which comprise basaltic-rocks clasts of various rock-types embedded in clay-sized pulverization paste, recognition of destruction fabric in them is difficult.

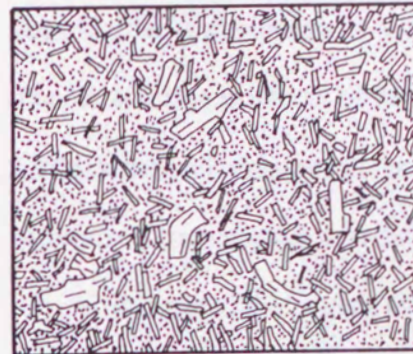
The destroyed basaltic rocks widely range in the size, fabric and volume of the destruction products. The weak, moderate, and strong destruction fabrics are herein defined by the approximate amount of the pulverization products. The weak, moderate, and strong destruction fabrics have the fine pulverization products of less than 5 %, 5 % to 30 %, and more than 30 % in amount, respectively (Fig. 14). In other words, the weak, moderate, and strong destruction fabrics are characterized by the predominance of brecciated rock-pieces larger than 2 mm, comminuted particles of 2 to 1/16 mm, and of pulverized materials less than 1/16, respectively.

1. Weak destruction fabric

The weak destruction fabric is characterized by narrow zones of pulverization and comminution products (Plate 15A, B). The primary constituents and texture of the parent rock of this variety have largely survived. Thus, the reconstruction of the parent rock-type is not difficult.

Interstices of coarsely brecciated rock-pieces are filled by pulverization products of finely pasted basaltic rocks with a small amount of comminuted phenocrysts. Some of plagioclases in the pulverization zone are little ruptured and remain euhedral. The pulverization zones in the crushed hyaloclastite consist entirely of clay-sized paste. The width of the interstices pulverization zone is notably varied, but most commonly less than 1 mm. Boundaries between the coarse rock-pieces and pulverization zones are

parent rock



— 1 mm

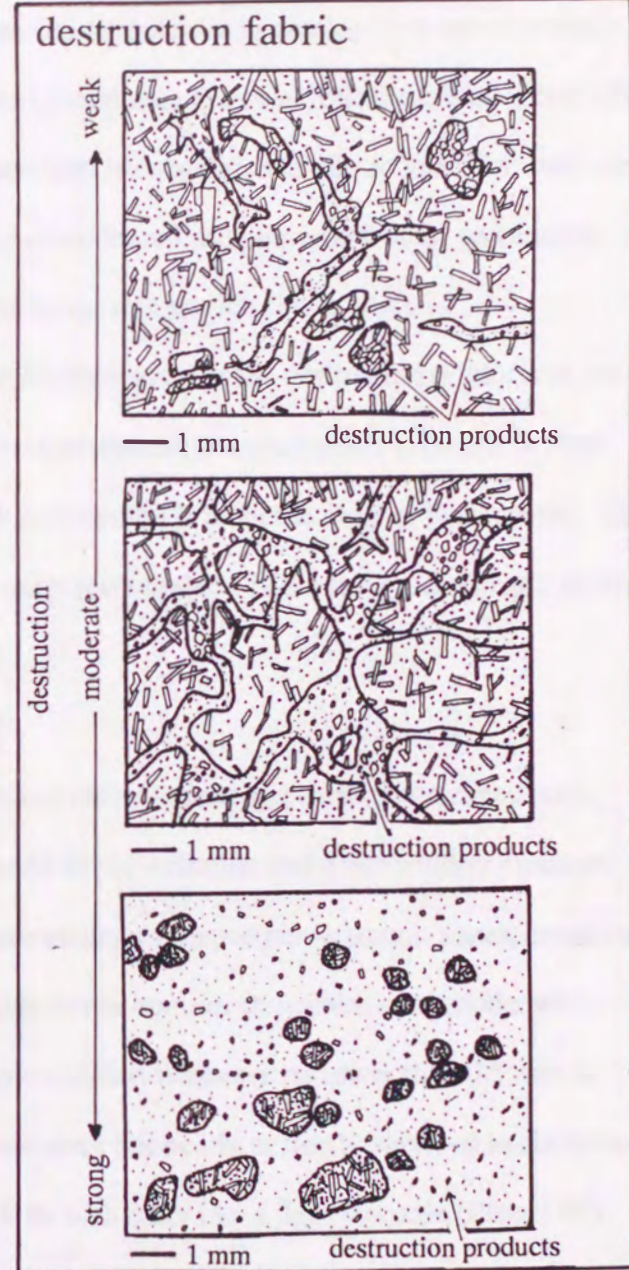


Fig. 14 Scheme showing the destruction fabrics of basaltic rocks from the weak to strong destruction stages.



indistinct, for the aphanitic groundmasses of rock-pieces are weakly pulverized along their peripheries.

The phenocrysts of plagioclase and pyroxene in the rock-pieces are selectively comminuted and pulverized, while the groundmass has been little destroyed (Plate 14). The destruction products of the phenocrysts are angular, and silt- to very fine sand-sized. Little destroyed phenocrysts, partially comminuted and pulverized ones, and entirely pulverized ones coexist in rock-pieces in one thin section (Plate 14A).

It is noted that a very small or no dislocation of the destruction products of the phenocrysts is discerned. All these broken phenocrysts are usually crowded to form small domains (Plate 14C, D) and no deformation in a ductile manner is discerned. The primary shape of the phenocrysts is easily recoverable. These facts mean nearly *in site* comminution of the phenocrysts.

2. Moderate destruction fabric

The moderate destruction fabric is characterized by coarsely brecciated rock-pieces of basalt lava with a small amount of pulverization and comminution products (Plate 15C, D). Brecciation and comminution, extensive pulverization zones, occasional dislocation of destruction products, and mortar textures characterize the moderate destruction fabric. In case that the pulverization zones are narrower than 0.5 mm in width, the primary cohesion of a parent rock has nearly perfectly survived in the coarsely brecciated rock-pieces, most of which fit each other like a jigsaw puzzle (Plate 15C). The network of pulverization zones forming mortar textures is commonly complicated, resulting in a fragmentation of rock-pieces into smaller sizes than in the moderate destruction fabric having the weak destruction fabric.

The brecciated and comminuted rock-pieces of basaltic lava are angular to

subrounded (Plates 15C). The outlines are usually irregularly rugged, and are in many cases difficult to be traced owing to the pulverization along the peripheries of brecciated rock-pieces.

An extensive pulverization area is composed of a large amount of clay-sized pulverized materials containing angular pulverization products of plagioclase (Plate 15D) and a small amount of coarse silt- to very fine sand-sized rock pieces (Plate 15C).

3. Strong destruction fabric

The strong destruction fabric is characterized by the dominance of very fine pulverization products with a small amount of comminuted rock-pieces (Plate 16A, B). The primary texture of the parent rocks has been almost totally lost and is hardly recoverable. Locally, however, some of rock-pieces are crowded together and can be easily reconstructed into a larger rock-piece (Plate 16A). The rocks appear to be a cataclasite, where the fine pulverized materials with scattered rock-pieces and comminuted particles are extensive. Even in this case, however, no distinct shear surfaces as considered to be characteristic of a cataclastic rock are identified.

The pulverized products are composed mainly of clay-sized, paste-like, cloudy destruction products derived most probably from aphanitic to glassy groundmasses of the parent and angular comminuted fragments of plagioclases and fine chips of basalt lavas less than medium silt-size, both of which are totally disorganized.

The rock-pieces of basalt are angular to subrounded, and pod, lenticular, and irregular in form. No positive indication for contamination of exotic components of basalt has been detected. Most of rock-pieces show a primary intersertal structure of the parent basalt, but its plagioclase laths are locally pulverized in a brittle manner. Outlines of the rock-pieces are sometimes indistinct due to pulverization of their marginal parts (Plate 16C). All comminuted rock-pieces are chaotically embedded in the fine

pulverization materials in many cases, but locally have a faint preferred orientation without an asymmetric deformation structure around rock-pieces indicating shear displacements.

B. Chaotic intermixing of oceanic-rock blocks of Suzuka unit

The Suzuka unit contains many mappable-sized blocks and smaller-sized blocks and clasts of Permian limestones, basaltic rocks, Permian chert, and Jurassic siliceous rocks (Fig. 3). The Permian limestone blocks are pod- and slab-shaped. Most of the limestone blocks are lithologically referable to the lower and middle members of the shallow-marine limestone succession (Fig. 5). The limestone blocks composed of limestone-breccia and redeposited limestone are also actually present, but sparse in occurrence and much smaller in size. A few of limestone blocks record an almost complete succession of the shallow-marine limestone. Most of the blocks retains parts of the entire succession.

Blocks of basaltic rocks are composed mainly of basalt lava with a small amount of dolerite, pyroclastic rocks, and hyaloclastite. Almost all the basaltic rocks have destruction fabrics of various style and degree. The blocks of basaltic rocks are variable in size, ranging from several centimeters to a few tens meters or more. The blocks are pod, lenticular, and slab in form. The outlines of the blocks of strongly pulverized basaltic rocks are highly complicated (Fig. 15).

Shapes of the Permian chert and Jurassic siliceous rocks are slab, pod, or lenticular. Some of the large blocks of the Jurassic siliceous rocks have the whole succession from chert to siliceous shale.

Blocks of these Permian and Jurassic oceanic rocks are totally disorganized and

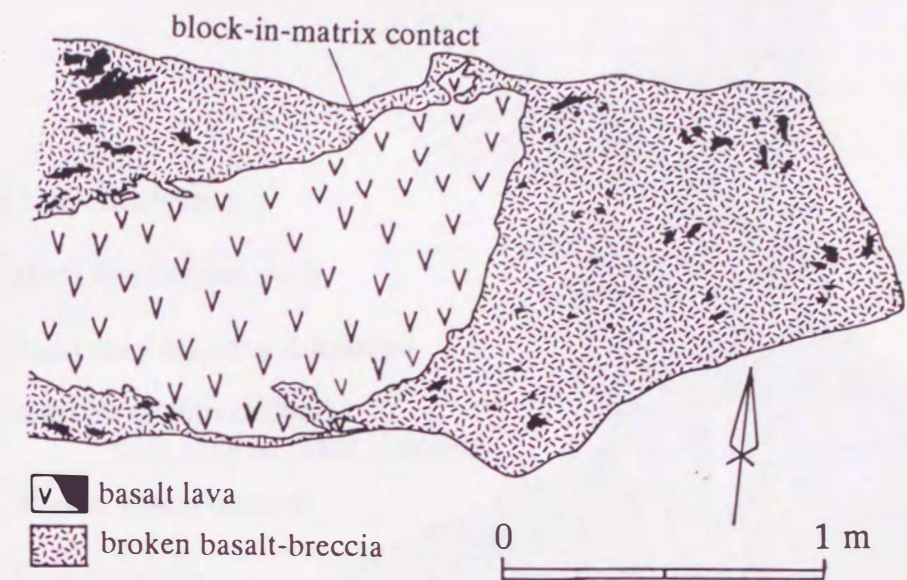


Fig. 15 A large block of destructed basalt lava embedded in broken basalt-breccia, in which much smaller clasts of basalt lava are scattered. Note that a large block of destructed basalt is in irregular-rugged and uneven contact with surrounding broken basalt-breccia. Locality is shown in Fig. 6.

orientation (Figs. 3, 16; Plate 19A, B). Even neighboring limestone blocks have different rock-types (Figs. 16, 17).

The blocks are in lithologically distinct, irregularly rugged and unshered contact with the surrounding broken basalt-breccias. However, the primary boundaries between blocks of basaltic rocks and broken basalt-breccia are locally obliterated because of the pulverization along the marginal parts of the blocks. Peripheries of the limestone blocks are locally injected by fine destruction products of the surrounding broken basalt-breccia.

The broken basalt-breccia is a newly introduced term, as defined in Plates 12 and 13, in order to denote a sedimentary breccia mainly consisting of clasts of basaltic rocks having the destruction fabrics with a small amount of clasts of Permian limestones, all of

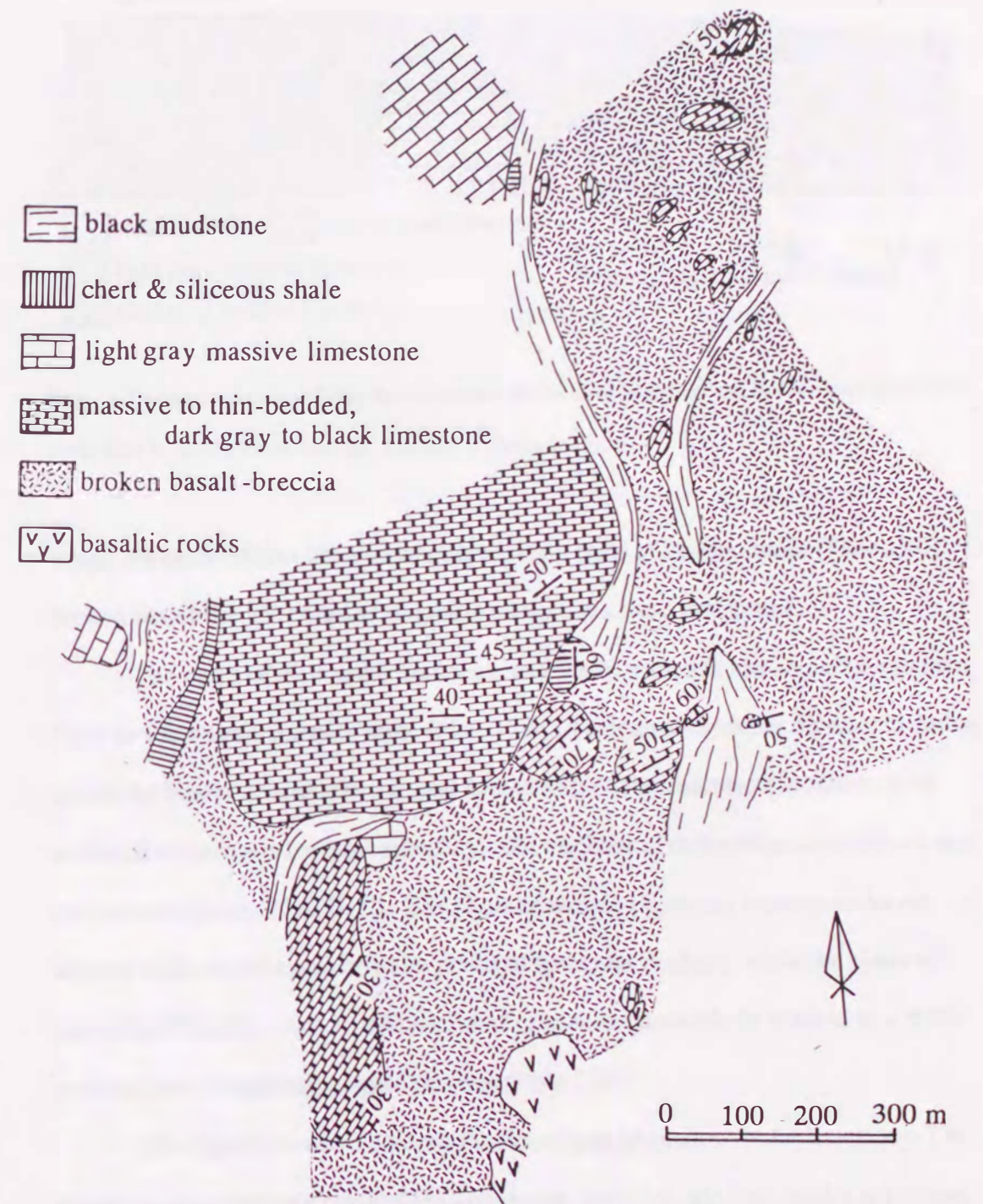


Fig. 16 Lithologic map illustrating chaotic occurrence of limestones of varied sizes embedded in broken basalt-breccia with elongated, narrow, laterally discrete tracts of terrigenous mudstone. Mapped area is shown in Fig. 6.

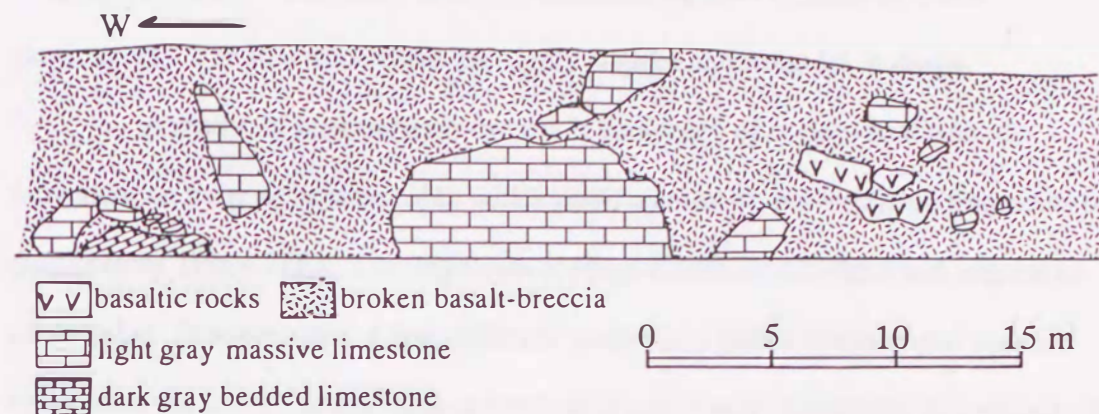


Fig. 17 Outcrop sketch showing the occurrence of blocks of limestone and basaltic rock chaotically embedded in broken basalt-breccia. Locality is shown in Fig. 6.

which are embedded in a matrix of pulverization paste of basaltic rocks (Plate 19C). The broken basalt-breccia contains no coarse terrigenous rocks and grains.

The clasts of the basaltic rocks are extremely varied in size, ranging less than 1mm to a few centimeters or more (Plate 17A). Their clast-types are diverse, including intersertal basalt, aphanitic basalt, and hyaloclastite. The microscopic observation reveals that the clasts having various styles of mechanical destruction coexist even in a thin-section (Plates 17A, B, C). The clasts of weakly destroyed basaltic rocks are angular to subangular and irregular pod, and lenticular in shape, while the clasts of pulverized basaltic rocks, in which laths of plagioclase are entirely crushed in a brittle manner, have irregularly rugged outlines (Plate 17B).

The limestone clasts comprise various types of shallow-water limestone. The dominant clast-types are peloidal lime-mudstone and bioclastic lime-mud/wackestone. All the clasts of limestones and limestone-breccia are referred to as the upper Lower Permian on the basis of the fusulines. The size of the limestone clasts widely varies, ranging from a few millimeters to several centimeters, most commonly a few

ranging from a few millimeters to several centimeters, most commonly a few centimeters. The limestone clasts are highly angular and irregular in shape.

A matrix of broken basalt-breccia is composed of a clay- to silt-sized pulverization paste of basaltic rocks with a small amount of pulverization fragments of plagioclases (Plate 17A). The fragments of plagioclases are silt-sized and angular to subangular. In some cases, a few, different grain-sized pastes of destroyed basaltic rocks form the matrix, where these pulverization pastes were complexly intermixed with one another in a ductile manner. Their boundaries between them are lithologically sharp and highly rugged (Plate 17B).

The clasts of basaltic rocks and limestone are in many cases completely disorganized and randomly oriented (Plate 17A). However, in case that the matrix is sparse, these clasts are densely packed and supported by each other (Plate 18A). The boundary between the matrix and limestone clasts is irregularly rugged and lithologically distinct (Plate 18A). The clasts of destructed basaltic rocks also are in lithologically distinct contact with the surrounding matrix of basaltic pulverization paste in spite of comminution and pulverization in them (Plate 17B).

The limestone clasts have been usually injected and fragmented into several rock-pieces by basaltic pulverization materials with pulverized plagioclases and minute rock-fragments of basaltic rocks (Plate 18B, C, D). The width of the injection abruptly changes. The injection is usually discontinuous laterally and fades out into the limestone clasts (Plate 18C). The pulverization pastes of the injections locally have a faint flow structure and embedded coarser destruction products of basalts and plagioclases have an indistinct preferred orientation (Plate 18D).